

**Title:** Unexpected growth of a classic yeast auxotroph

**Authors:** S. Branden Van Oss<sup>1,2,7</sup>, Saurin Bipin Parikh<sup>1,2,7</sup>, Nelson Castilho Coelho<sup>1,2,7</sup>, Aaron Wacholder<sup>1,2</sup>, Ivan Belashov<sup>3</sup>, Manuel Michaca<sup>1,2</sup>, Jiazhen Xu<sup>1</sup>, Yun Pyo Kang<sup>4,5</sup>, Katherine M. McCourt<sup>1,2</sup>, Jake McKee<sup>1</sup> Trey Ideker<sup>6</sup>, Andrew P. VanDemark<sup>3</sup>, Gina M. DeNicola<sup>4</sup>, Anne-Ruxandra Carvunis<sup>1,2,\*</sup>

<sup>1</sup>Department of Computational and System Biology, University of Pittsburgh School of Medicine, Pittsburgh, Pennsylvania, 15213

<sup>2</sup>Pittsburgh Center for Evolutionary Biology and Medicine, University of Pittsburgh School of Medicine, Pittsburgh, Pennsylvania, 15213

<sup>3</sup>Department of Biological Sciences, University of Pittsburgh, Dietrich School of Arts & Sciences, Pittsburgh, Pennsylvania, 15213

<sup>4</sup>Department of Cancer Physiology, H. Lee Moffitt Cancer Center, Tampa, Florida, 33612

<sup>5</sup>College of Pharmacy and Research Institute of Pharmaceutical Sciences, Seoul National University, Seoul, Republic of Korea (current address)

<sup>6</sup>Departments of Medicine, Bioengineering, Computer Science and Engineering, Institute for Genomic Medicine, University of California San Diego, La Jolla, California, 92093

<sup>7</sup>Co-first author: These authors contributed equally

\*Correspondence: [anc201@pitt.edu](mailto:anc201@pitt.edu)

**Keywords:** auxotrophy, methionine, hydrogen sulfide, sulfur, metabolism

**Corresponding Author:**

Dr. Anne-Ruxandra Carvunis

Department of Computational and Systems Biology

Pittsburgh Center for Evolutionary Biology and Medicine

University of Pittsburgh School of Medicine

3501 Fifth Avenue

Pittsburgh, PA 15260, U.S.A.

Phone: +1 (412) 648-3335

Email: [anc201@pitt.edu](mailto:anc201@pitt.edu)

## ABSTRACT

In budding yeast, the Met15 enzyme has long been assumed to be the sole homocysteine synthase, facilitating *de novo* synthesis of sulfur-containing organic compounds (organosulfurs) from inorganic precursors. Here we show that an alternative homocysteine synthase encoded by the previously uncharacterized gene *YLL058W* supports growth of mutants lacking *MET15* in the absence of exogenous organosulfurs. This growth is observed specifically when cells are deposited in an automated fashion to seed colonies, but not with traditional cell propagation techniques such as thick patches of cells or liquid cultures. We show that the lack of growth in these contexts, which has historically justified the status of *MET15* as a classic auxotrophic marker, is largely due to toxic levels of hydrogen sulfide accumulation rather than an inability to perform *de novo* homocysteine biosynthesis. These data have broad implications for investigations of sulfur starvation/metabolism, including studies of aging and emerging cancer therapeutics.

## INTRODUCTION

The metabolism of organic sulfur-containing compounds (“organosulfurs”) is critical for all domains of life. There exists substantial diversity among the enzymes and other components of the cellular networks that govern this metabolism. This diversity is particularly true of plants and microbes which, unlike animals, can synthesize organosulfurs from inorganic sulfates via the sulfate assimilation pathway (SAP) (Thomas and Surdin-Kerjan, 1997). Enzymes in the SAP reduce inorganic sulfates into sulfides and, in the terminal step, generate homocysteine from O-acetyl-L-homoserine (OAH) and hydrogen sulfide (H<sub>2</sub>S). In *Saccharomyces cerevisiae*, the Met15 enzyme (also referred to as Met17 and Met25) catalyzes this reaction both *in vivo* (Masselot and De Robichon-Szulmajster, 1975) and *in vitro* (Chen et al., 2018; Yamagata, 1971). Homocysteine can then be converted either directly to methionine or indirectly to cysteine via a cystathionine intermediate. These amino acids may be incorporated into nascent polypeptide chains; alternatively, they may be further modified to produce other essential organosulfurs with critical regulatory roles, including the “universal methyl donor” S-adenosylmethionine (SAM) and glutathione, an important buffer against oxidative stress. Reactions downstream of homocysteine biosynthesis are reversible, and thus all of these organosulfurs may also be recycled back to homocysteine (Thomas and Surdin-Kerjan, 1997).

The first precise and complete deletion of *MET15* (*met15Δ0*) in *S. cerevisiae* was made in 1998, in the S288C strain background, as part of a collection of “designer deletion” strains containing one or more deletions of common *S. cerevisiae* auxotrophic markers

(Brachmann et al., 1998). A large number of commonly used laboratory strains contain the *met15Δ0* mutation, including BY4741, which serves as the genetic background of the haploid *MATa* version of the yeast deletion collection that has been extensively utilized for functional genomics and other purposes (Giaever and Nislow, 2014). Notably, the use of this deletion as an auxotrophic marker by yeast geneticists and the corresponding assumption that *MET15* is required for growth in organosulfur-free media has been applied to the interpretation of a wide range of studies of sulfur metabolism in *S. cerevisiae* (Johnson and Johnson, 2014; Plummer and Johnson, 2019; Zou et al., 2017).

There are, however, data suggesting that *MET15* may not be strictly required for growth in the absence of exogenous organosulfurs. *MET15* was first identified in a screen for resistance to the toxic compound methylmercury (Singh and Sherman, 1974). In this study, *met15* mutants were shown to be auxotrophic for methionine and resistant to methylmercury, but, at a critical concentration of methylmercury, the methionine requirement appeared to be alleviated, and these mutants were isolated at high frequency from selection medium lacking organosulfurs. There have also been anecdotal reports of papillae seen when replica plating thick patches of *met15Δ0* cells to medium lacking organosulfurs (Boeke Lab, 2003).

Additionally, there is reason to believe that our knowledge of *S. cerevisiae* sulfur metabolism may be incomplete. The transcriptional regulation of genes in the sulfur metabolic network has been well-described, with Met4 being the sole known

transcriptional activator of the network (Thomas and Surdin-Kerjan, 1997). Of the 45 genes that compose the Met4 “core regulon” (Lee et al., 2010), three are classified by the Saccharomyces Genome Database (SGD) as “uncharacterized,” and four of the 42 verified genes have functions described as “unknown” or “putative” (Stanford University, 2020). One of the uncharacterized genes, *YLL058W*, is not associated with organosulfur auxotrophy or any other known phenotypes upon deletion, but shares sequence similarity with the cystathionine  $\gamma$ -synthase *STR2* (Zhang et al., 2001), and earlier studies (Lee et al., 2010; Zhang et al., 2001) have hinted at the fact that it may play a role in sulfur metabolism.

Here, we show stable growth of *met15 $\Delta$*  cells propagated via automated colony transfer in media lacking exogenous organosulfurs. This stable growth requires the presence of exogenous inorganic sulfates and an intact SAP, as well as the uncharacterized gene *YLL058W*. We demonstrate that *Yll058w* can catalyze the synthesis of homocysteine directly from OAH and H<sub>2</sub>S in a purified *in vitro* system, albeit at a lower efficiency than Met15. Hence, *met15 $\Delta$*  cells are able to synthesize organosulfurs from inorganic sulfates despite a long-held assumption of the contrary. Our observations suggest that the ability of *met15 $\Delta$*  cells to grow in the absence of exogenous organosulfurs is context-dependent and highly sensitive to the manner in which the cells are propagated. Specifically, stable growth is observed with automated colony transfer, but very low or no growth is observed using “conventional” techniques such as thick patches or liquid cultures, leading to the appearance of auxotrophy. We show that this appearance of auxotrophy is at least partially explained by toxic levels of accumulated H<sub>2</sub>S,

presumably due to the lower enzymatic efficiency of YII058w relative to Met15. The addition of an H<sub>2</sub>S chelator to media lacking organosulfurs partially rescues the growth of *met15Δ* cells propagated in thick patches or liquid media. Our results demonstrate the existence of an alternative pathway for homocysteine production in *S. cerevisiae*. These results have implications for a broad range of studies that presume organosulfur auxotrophy in *met15Δ* cells, as well as for our understanding of sulfur metabolism more generally.

## RESULTS

### ***met15Δ* cells show unexpected growth in the absence of external organosulfurs**

The *met15Δ0* deletion has been examined extensively in BY4741, a strain commonly used as a “wild type” control for genome-scale deletion and overexpression screens (Douglas et al., 2012; Giaever and Nislow, 2014). We serendipitously observed robust growth of BY4741 when cells pinned in a 384-colony array (**Figure 1A, Table S1**) were transferred from a rich medium (YPDA) to a “synthetic defined” (SD) medium lacking methionine (Met) and cysteine (Cys) and containing glucose as the carbon source (hereafter referred to as “SD-Met+Glu”). Interestingly, over ~5 days, the morphology of *met15Δ0* colonies was markedly different than that of *MET15<sup>+</sup>* colonies (**Figure S1**). We first made these observations using a BY4741 control strain from the haploid *MATa* deletion collection; this strain has a *KanMX* cassette in its genome that confers resistance to the antibiotic G418. To confirm that this surprising finding was not unique to our particular copy of this strain or related in some way to the presence of the *KanMX* cassette, we purchased BY4741 (lacking the *KanMX* cassette) and BY4742 (to serve as a *MET15<sup>+</sup>* control) from a commercial vendor (Dharmacon) and repeated this assay (**Figure 1B**), using the commercial strains to create glycerol stocks containing four biological replicates. BY4741 cells again grew on SD-Met+Glu, although the resulting colonies were smaller in size than those formed by the BY4742 strain on the same medium (effect size = 0.341, p-value = 0.021 [Kruskal-Wallis test]; **Figure 1B-C**). Both BY4741 and BY4742 harbor complete deletions of *URA3* and *LEU2* (Brachmann et al., 1998), rendering them auxotrophic for uracil (Ura) and leucine (Leu). There was a large,

statistically significant difference in relative colony size between BY4741 colonies that formed on SD-Met+Glu and the very small colonies detectable on SD-Ura+Glu or SD-Leu+Glu (effect size = 0.627, p-value = 0.021 [Kruskal-Wallis test] and effect size = 0.757, p-value = 0.007 [Kruskal-Wallis test], respectively). Our experiments reveal that, in this automated colony transfer procedure, BY4741 does not exhibit the dramatically reduced growth associated with auxotrophy on SD-Met+Glu medium, despite lacking *MET15*.

Given the longstanding assumption of organosulfur auxotrophy in *met15Δ* strains, we took several steps to confirm the above observation. First, to ensure that our media were devoid of organosulfur contamination, we analyzed both SD-Met and SD+Met media by mass spectrometry, as well as the individual components of said media. We specifically looked for methionine, cysteine, homocysteine and S-adenosylmethionine. With the expected exception of methionine in the SD+Met sample, none of these compounds were detected (**Table S2**). To rule out the possibility that a secondary mutation drove the growth of BY4741 colonies, we next performed a cross between BY4741 and BY4742, dissected eight four-spore tetrads, and patched them to individual SD-Met+Glu agar plates to prevent cross-feeding. We observed 2:2 segregation with respect to the growth phenotype in all eight tetrads, as expected for a monogenic phenotype (**Figure S2**). The growth of thick BY4741 patches was extremely weak, consistent with an organosulfur auxotrophy and in contrast to that observed with the pinned colonies. Thus, the unexpected growth of BY4741 cells lacking *MET15* on

organosulfur-free media was dependent on the manner in which the cells were propagated.

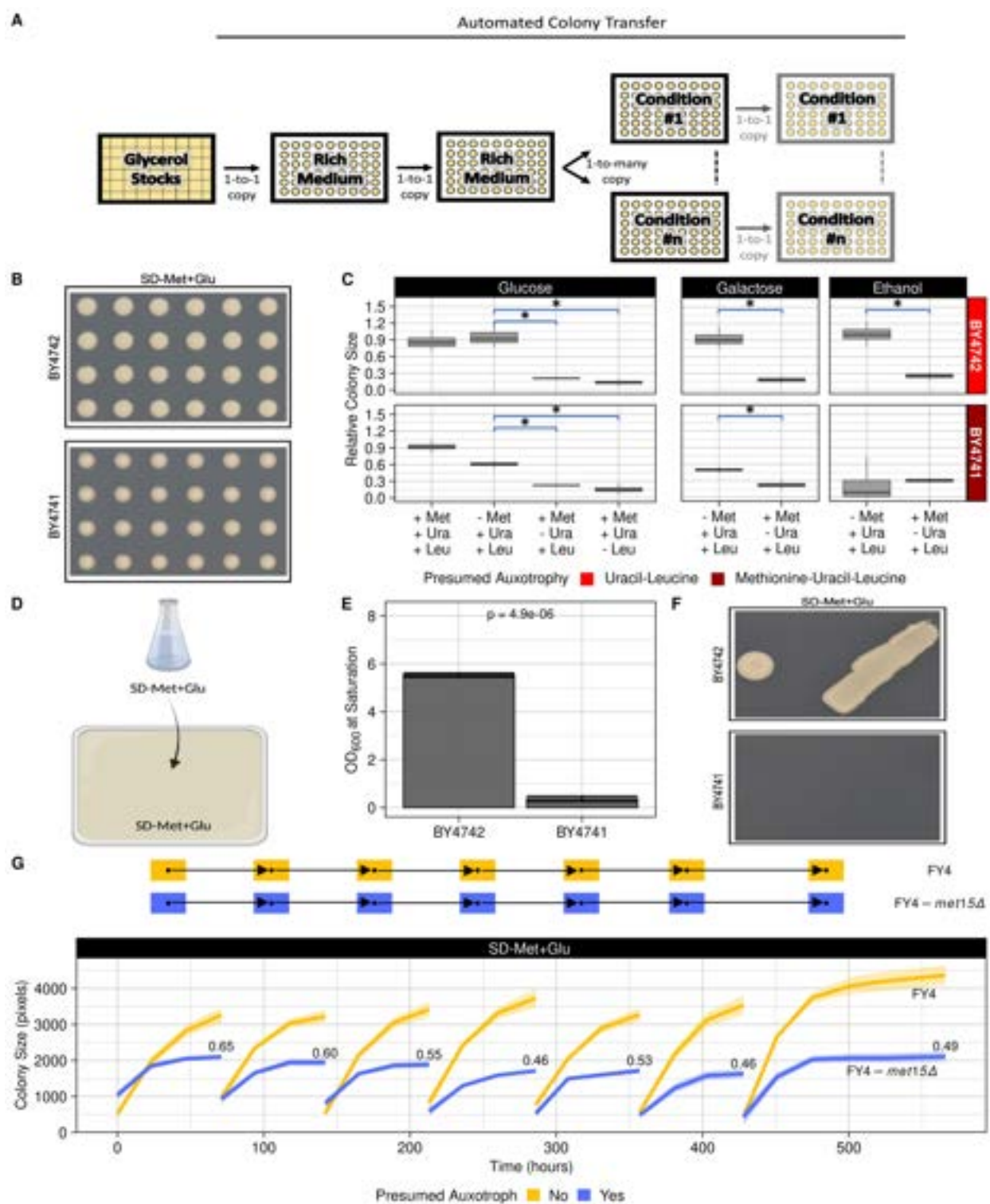


**Figure 1. The unexpected growth of *met15Δ* cells on organosulfur-free media is both stable and context-dependent.** **A)** Generalized schema depicting the automated colony transfer technique used throughout the study to evaluate the growth of individual strains in various media conditions. Glycerol stocks at 384-well density for each strain tested in this manner were made, each containing 96 technical replicates of 4 unique biological replicates obtained from individual single colonies; border colonies were excluded from the colony size analysis, leaving 77 technical replicates of each biological replicate per plate; see **Experimental Procedures** for a more detailed description of the stock construction protocol. Cells were pinned with the RoToR HDA robot as described in **Experimental Procedures** and **Table S1** from glycerol stocks to “starter” agar plates containing rich medium (YPDA), allowed to grow to saturation, pinned from these starter plates again to YPDA plates (to ensure a roughly homogenous colony size), and then pinned to plates containing the various “condition” media. For the experiments depicted in **Figures 1B-C, 2B-D, and 3D**, and the related Supplementary Figures, cells were transferred to the condition plate a single time; for the experiments depicted in **Figures 1G and 2E**, cells were repinned to the indicated condition media multiple times (light gray plates) as described in the accompanying schema and text. **B)** Unexpected growth of a strain harboring the *met15Δ0* deletion (BY4741) on a medium lacking organosulfurs (SD-Met+Glu). Although the colonies were smaller than those formed by the *MET15<sup>+</sup>* BY4742 strain (top), the robust growth of the BY4741 strain lacking *MET15* (bottom), under what has previously been considered an auxotrophic condition, was not anticipated. See **Supplementary Material** for a complete genotype of both strains. Cropped images of representative 384-density plates are shown. Colonies shown here have grown for 366 hours at 30°C. **C)** Robust growth of *met15Δ0* cells on SD-Met+Glu and SD-Met+Gal, but not on SD-Met+EtOH. Box plots show the relative colony size distribution (y-axis) at saturation (~358 to 366 hours) of BY4742 and BY4741 grown at 30°C on “SD” media with various carbon sources containing or lacking the indicated nutrients (x-axis). Data associated with each plot is drawn from two 384-colony density plates for each strain, made and grown as described in Panel A. Pixel counts for each colony were normalized to the median colony size for a prototrophic strain (FY4) grown in the same conditions (**Figure S4B**) to obtain a relative colony size (**Experimental Procedures**). Statistical significance was calculated with the Kruskal-Wallis test, using the median colony sizes of all the biological replicates. Relevant significant comparisons (p-value < 0.05) are denoted using a blue horizontal line and an asterisk. The unexpected growth of BY4741 colonies was observed when glucose or galactose, but not ethanol, comprised the carbon source. **D)** Schema depicting the experimental setup for the data presented in Panels E and F. Three biological replicates of each strain were grown in individual Erlenmeyer flasks in SD-Met+Glu liquid medium at 30°C. After ~51 hours, 10 μl drops taken from these cultures were then used to make spots or patches on solid SD-Met+Glu medium (**Experimental Procedures**). **E)** BY4741 cells fail to grow in liquid SD-Met+Glu medium. The bar graphs show the mean optical density at 600nm (OD<sub>600</sub>, y-axis) that was measured for each strain (x-axis) on a spectrophotometer following incubation for ~51 hours at 30°C. Error bars indicate standard error. Statistical significance, shown on top, was calculated using a two-tailed Student’s T-test. **F)** BY4741 cells also fail to grow on solid SD-Met+Glu medium in large spots or patches. Ten μl drops from each liquid culture from Panel E were spotted and struck to SD-Met+Glu solid agar medium and incubated at 30°C for 192 hours, and then imaged. Cropped representative images are shown. BY4742 (top) grew as expected, while BY4741 (bottom) failed to grow, consistent with its characterization as an organosulfur auxotroph. **G)** Growth of FY4-*met15Δ* on an organosulfur-free medium is stable. For both strains (FY4 and FY4-*met15Δ*), the initial pinning steps (glycerol stock → YPDA → YPDA) were as described in Panel A. Plates containing 384 colonies of a single strain were then pinned from YPDA to SD-Met+Glu, grown for the indicated number of hours at 30°C, and then transferred from and to SD-Met+Glu plates six additional times as represented in the schema at the top of the panel. Solid lines represent the median colony size at each time point, with the shaded area corresponding to one standard deviation. Border colonies and outliers (defined as colonies >2 median-adjusted deviations from the median colony size) were removed from the analysis. Numbers displayed in black next to the blue curves correspond to the fitness of FY4-*met15Δ* relative to FY4 as determined by dividing the median colony size at the final time point of each pinning.

To further investigate the dependence of this growth phenotype on the cell propagation technique used, we inoculated BY4741 and BY4742 in liquid SD-Met+Glu medium in culture flasks (**Figure 1D**). In this context, BY4742 cultures grew normally, while very little growth was seen in BY4741 cultures (**Figure 1E**). We then used 10  $\mu$ l drops taken from these liquid cultures to make spots and patches on SD-Met+Glu solid medium (**Figure 1D**). Here again we observed normal growth of BY4742 cells, but no growth of BY4741 cells (**Figure 1F**). Thus, BY4741 displayed the expected auxotrophic-like phenotypes when using conventional cell propagation techniques, but not when using automated colony transfer.

We next sought to determine the extent to which the unexpected growth of *met15* $\Delta$  colonies depended on the specific composition of the growth medium, beginning with the carbon source utilized by the cells. We repeated the automated colony transfer procedure using SD-Met media with either galactose (SD-Met+Gal) or ethanol (SD-Met+EtOH) as the sole carbon source instead of glucose (**Figure 1C**). Similar to our observations in SD-Met+Glu, BY4741 cells grew when galactose was used as a carbon source, and BY4741 colonies grew to much larger sizes on SD-Met+Gal than on SD-Ura+Gal (effect size = 0.561, p-value = 0.021 [Kruskal-Wallis test]). In contrast, very little growth of BY4741 was seen on SD-Met+EtOH; on this medium, growth was consistent with auxotrophy, slightly weaker than that observed on SD-Ura+EtOH medium. We also asked whether the unexpected growth of *met15* $\Delta$  colonies depended on the absence of certain external amino acids on the SD-Met medium by repeating the pinning procedure using “synthetic complete” (SC) medium containing all amino acids except Met and Cys

(SC-Met-Cys). We observed growth similar to that seen on SD-Met, whether glucose or galactose was used as a carbon source (relative to BY4742, effect size = 0.171, p-value = 0.021 [Kruskal-Wallis test] and effect size = 0.454, p-value = 0.021 [Kruskal-Wallis test]), respectively; **Figure S3**). As was the case with SD media, the growth of BY4741 colonies on SC-Leu+Glu was substantially weaker than what was observed on SC-Met-Cys+Glu (effect size = 0.914, p-value = 0.007 [Kruskal-Wallis test]).

The BY4741 strain harbors several auxotrophies engineered for laboratory use (see **Experimental Procedures** for the complete genotype) (Brachmann *et al.*, 1998). To study the specific consequences of *MET15* loss, we utilized CRISPR to make a scarless deletion of *MET15* in the prototrophic FY4 background (FY4-*met15*Δ) (**Experimental Procedures**) and used this strain for all subsequent experiments. Using the same automated colony transfer procedure, we examined the growth of this mutant on SD-Met medium containing glucose, galactose, or ethanol as the sole carbon source, and on SC-Met-Cys medium with either glucose or galactose as the sole carbon source. The growth of FY4-*met15*Δ cells was similar to that observed for BY4741 cells. We again observed robust growth on SD-Met when glucose or galactose, but not ethanol, were used as the sole carbon source (**Figure S4**). Furthermore, FY4-*met15*Δ grew to similar colony sizes as BY4741 on SC-Met-Cys medium, whether glucose or galactose was used as a carbon source (**Figure S3**). Thus, the unexpected growth of cells lacking *MET15* on organosulfur-free media was not dependent on the genetic background particular to the BY4741 strain.

We next considered two potential explanations for the surprising growth of *met15Δ* colonies on media lacking organosulfurs. First, it may reflect *de novo* homocysteine biosynthesis through an alternative enzyme or pathway. Second, it may be due to the recycling of preexisting organosulfurs within cells and/or scavenging of the same from dead cells or from neighboring colonies. To distinguish between these possible explanations, we repeated the pinning procedure described in **Figure 1A** with FY4 and the FY4-*met15Δ*, this time pinning from and to SD-Met+Glu six consecutive times following the initial pinning from YPDA. We measured the colony size at semi-regular intervals to obtain growth curves. The FY4-*met15Δ* strain displayed robust growth on SD-Met+Glu over repeated pinnings (**Figure 1G**). Relative to FY4, the fitness of these colonies (determined by dividing the median colony size at the final time point of each pinning) was 0.65 on the initial SD-Met+Glu plates and decreased only slightly over the course of six successive pinnings to SD-Met+Glu, stabilizing at ~0.50. The amount of new biomass generated throughout this repeated pinning experiment demonstrates that the growth of FY4-*met15Δ* cells is a stable phenomenon that cannot be explained by recycling or scavenging.

Our observations show that, despite a longstanding assumption of auxotrophy, *met15Δ* strains can in fact grow stably in media lacking external organosulfurs. This growth is context-dependent, manifesting when cells are grown in pinned colonies, but not in thick patches or liquid cultures, and when cells utilize glucose or galactose, but not ethanol, as a carbon source.

## **Stable growth of *met15Δ* cells on organosulfur-free media is dependent on the utilization of inorganic sulfates and is not seen in other presumed auxotrophs**

We next investigated whether the unexpected growth of *met15Δ* colonies that we observed in our automated colony transfer assay was specific to *met15Δ* mutants, or whether it would also be found in other mutants presumed to be unable to grow on organosulfur-deficient media. To do so, we again utilized CRISPR to make complete deletions in the FY4 background of nine additional genes encoding enzymes involved in the organosulfur biosynthesis (**Figure 2A**). These mutants, along with FY4 and the FY4-*met15Δ* strain, were transferred as described above (**Figure 1A**) from 384-density YPDA plates to either YPDA or SD-Met+Glu.

For eight of the nine deletion strains, we observed growth in SD-Met+Glu that was consistent with the known roles of the deleted genes in the organosulfur biosynthesis pathway (**Figure 2A**). Met5 and Met10 form a complex which acts as a sulfite reductase, catalyzing the terminal reaction in the SAP (Masselot and De Robichon-Szulmajster, 1975). Met2 is thought to be required for all *de novo* organosulfur biosynthesis. Both Met6 and Met13 are essential for the biosynthesis of methionine (Masselot and De Robichon-Szulmajster, 1975). Cys4 has similarly been shown to be required for the biosynthesis of cysteine (Ono et al., 1988). In agreement with these findings, the FY4-*met5Δ*, FY4-*met10Δ*, FY4-*met2Δ*, FY4-*met6Δ*, FY4-*met13Δ*, and FY4-*cys4Δ* strains all displayed negligible or no growth on SD-Met+Glu (effect sizes = 0.887, 0.869, 0.930, 0.904, 0.903, and 0.981, respectively; p-value < 0.05 [Kruskal-Wallis test] for all comparisons) (**Figure 2B**). Loss of the *STR3* gene renders cells unable to utilize

cysteine or glutathione as a sole sulfur source (Hansen and Johannesen, 2000); however, the extent to which this mutant can utilize sulfates has not, to our knowledge, been directly examined. *MET12* is a paralog of *MET13*, but its deletion has not been associated with any *in vivo* phenotypes. The FY4-*str3Δ* strain had a moderate growth defect in SD-Met+Glu that was also observed in YPDA, while the FY4-*met12Δ* strain grew normally (**Figure 2B**).

Similar to what we have observed for Met15 (**Figures 1 and 2B**), we observed a surprising growth phenotype for cells lacking the ATP sulfurylase Met3. Met3 sits at the top of the sulfate assimilation pathway (SAP), catalyzing the first step in the reduction of intracellular sulfate, and is thought to be essential for growth when unreduced sulfates are the sole sulfur source (Masselot and De Robichon-Szulmajster, 1975). However, the FY4-*met3Δ* mutant, which grew normally on YPDA, displayed growth on SD-Met+Glu that was roughly equivalent to that seen with the FY4-*met15Δ* strain (relative to FY4, effect size = 0.651, p-value < 0.001 [Kruskal-Wallis test] and effect size = 0.618, p-value < 0.001 [Kruskal-Wallis test], respectively; **Figure 2B**). Unlike *met15Δ* strains however, the growth of the FY4-*met3Δ* mutant was largely unaffected by carbon source, with only a slightly greater growth defect in SD-Met+Gal and SD-Met+EtOH than in SD-Met+Glu (effect size = 0.289, p-value = 0.021 [Kruskal-Wallis test] and effect size = 0.298, p-value = 0.021 [Kruskal-Wallis test] respectively, **Figure S5**).

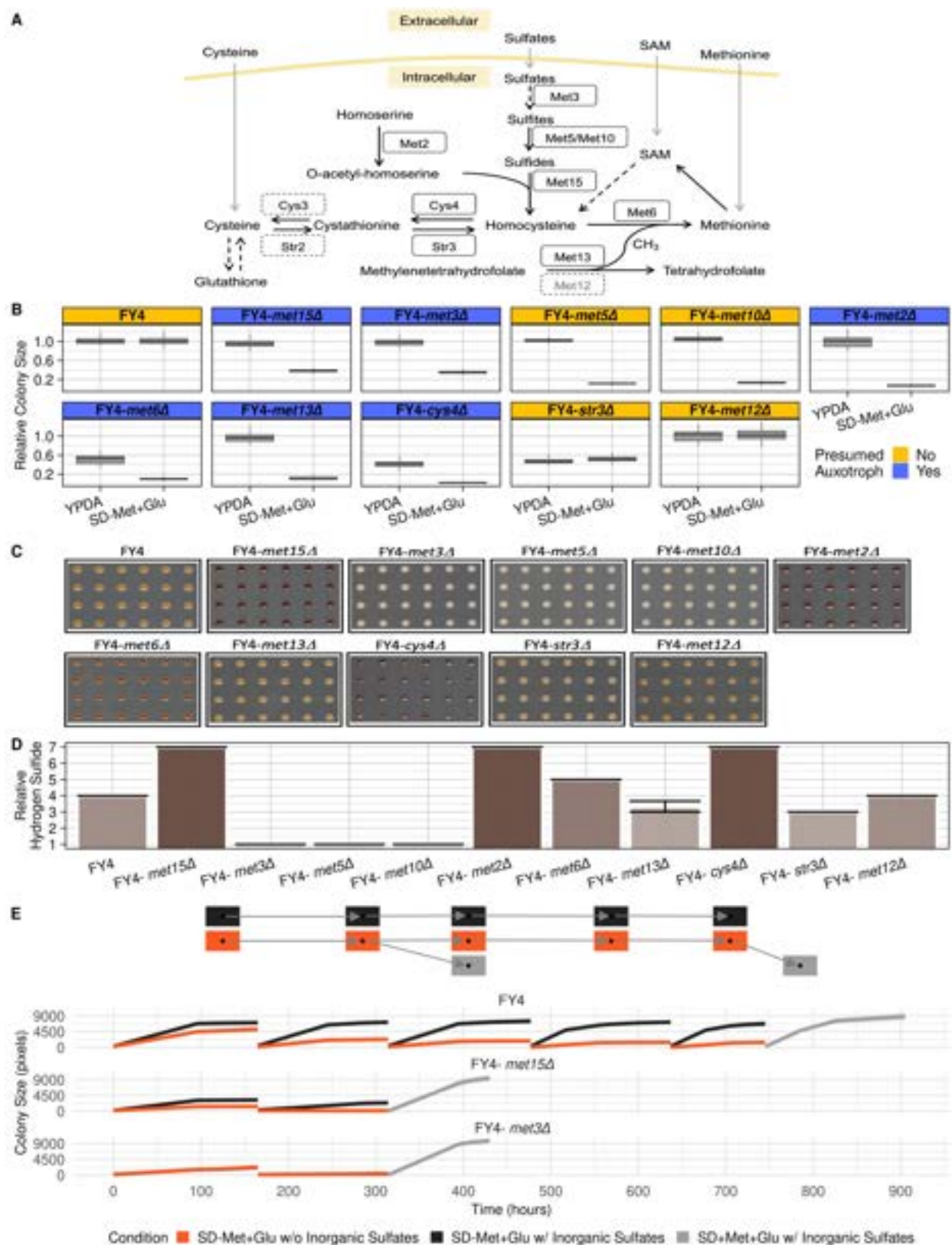


**Figure 2. Growth of *met15Δ* colonies in organosulfur-free media is specific and dependent on the utilization of inorganic sulfates. A)** The organosulfur biosynthesis pathway in *S. cerevisiae*. If present in the growth medium, external organosulfurs such as methionine, cysteine, and S-adenosylmethionine (SAM) can be directly imported (gray arrows); inorganic sulfur in the form of sulfates can also be imported and reduced to sulfides via the sulfate assimilation pathway. Sulfides are converted into organosulfurs through the activity of the Met15 enzyme, which catalyzes the production of homocysteine from sulfides and O-acetyl-homoserine. Homocysteine is then converted to numerous critical downstream organosulfurs, including the proteinogenic amino acids methionine and cysteine, the “universal methyl donor” SAM, and glutathione, one of the major cellular buffers against oxidative stress. A selection of critical compounds in the pathway are indicated. Enzymes are indicated next to the reactions they catalyze, which are illustrated with arrows that indicate reaction directionality. Full black arrows correspond to a single reaction and dashed arrows indicate that multiple steps are depicted. The growth of strains lacking the enzymes depicted within solid boxes on an organosulfur-deficient medium is examined in Panel B, while other key enzymes in the pathway are depicted within dashed boxes. The *in vivo* biosynthesis of methionine requires the activity of two enzymes – the methionine synthase Met6, and the methylenetetrahydrofolate reductase Met13, which provides the methyl group. The Met13 isozyme Met12 (shown in gray) is active *in vitro*, but its loss is not associated with any *in vivo* phenotype (Raymond et al., 1999). Drawing inspired by (Walvekar and Laxman, 2019). **B)** *met3Δ* cells also show unexpected growth. For each strain and condition, the pinning procedure and plate construction was as described in **Figure 1A** and **Experimental Procedures**. Box plots show the growth of the prototrophic FY4 control strain and mutant strains in the FY4 background with genes encoding enzymes with a known role in organosulfur biosynthesis deleted by means of CRISPR, on rich medium (YPDA, left) and on medium lacking organosulfurs (SD-Met+Glu, right) at 30°C. The box plots show colony size (pixel count, y-axis) data for two 384-colony density plates per strain (subpanels), containing four biological replicates that each have 77 technical replicates (after edges are excluded). The average pixel count at saturation (~160-173.5 hours in SD-Met+Glu; 83.5-89 hours in YPDA) was normalized to FY4 to obtain a relative colony size. **C-D)** Disruptions of the organosulfur biosynthesis pathway result in a range of hydrogen sulfide (H<sub>2</sub>S) accumulation in cells. Images (Panel C) and qualitative assessment of relative H<sub>2</sub>S (Panel D) in the same strains from Panel A pinned to rich medium containing bismuth (BiGGY; see **Supplementary Material**). The amount of bismuth precipitate formed, reflected in the relative darkness of the colonies, is a proxy for H<sub>2</sub>S levels in the cell (Nickerson, 1953). The qualitative assessment involved two replicates scored by eye in duplicate by independent observers on a scale of 1-7, with the darkest strain(s) assigned a value of seven and the lightest strains assigned a value of one. Bars indicate standard error. **E)** Growth of FY4-*met15Δ* colonies requires inorganic sulfates. The indicated strains were grown either on our “standard” SD-Met+Glu medium (containing inorganic sulfates) or on an analogous medium completely devoid of inorganic sulfates (see **Experimental Procedures** and **Supplementary Material** for details). After reaching saturation on these “condition” plates, all strains were pinned to the same condition a second time. The FY4-*met15Δ* and FY4-*met3Δ* strains, which failed to show appreciable growth after the second pinning, were then pinned from SD-Met+Glu without inorganic sulfates to SD+Met+Glu with inorganic sulfates. In the case of FY4, cells were pinned five times to SD-Met+Glu without inorganic sulfates before pinning to SD+Met+Glu with inorganic sulfates. This experimental procedure is indicated in the schema at the top of the panel. Beneath the schema are growth curves of the indicated strains (subpanels) through the entire experimental procedure with the mean colony size (solid lines) and one standard deviation (shaded region) depicted. The colony size (pixel count) data used to make the growth curves comes from two 384-colony density plates per strain, containing four biological replicates that each have 77 technical replicates (after edge colonies are excluded). Each media condition is represented by a different color as indicated at the bottom of the panel: orange for SD-Met+Glu without inorganic sulfates, black for SD-Met+Glu with inorganic sulfates, gray for SD+Met+Glu with inorganic sulfates. The orange and black curves in the lower subpanel (FY4-*met3Δ*) overlap.

This surprising growth of *met3Δ* cells, which according to the known metabolic pathway (**Figure 2A**) should be unable to convert inorganic sulfates to sulfides, led us to

examine the level of free sulfides present in our mutant strains. To do so we utilized an established colony color assay using bismuth. Bismuth reacts with free sulfides to form a dark precipitate on the surface of cells, the darkness of which roughly corresponds to the amount of excess sulfides in the cell (Nickerson, 1953). This color phenotype is therefore a proxy for *de novo* homocysteine biosynthesis through the canonical pathway, with strains deficient in this activity expected to accumulate sulfides and form darker colonies. This assay also functions as a proxy readout for the activity of the SAP, where a broken or inefficient pathway would be expected to result in little to no free sulfide accumulation and lighter colonies. The FY4-*met15* $\Delta$  and FY4-*met2* $\Delta$  mutants both formed very dark colonies when grown on complete media containing bismuth (BiGGY), confirming that they are deficient in homocysteine biosynthesis through the canonical pathway. The FY4-*cys4* $\Delta$  mutant also formed very dark colonies, consistent with the well-documented upregulation of the SAP that occurs when cells cannot make cysteine (Hansen and Johannesen, 2000). The FY4-*met6* $\Delta$ , FY4-*met13* $\Delta$ , and FY4-*str3* $\Delta$  mutants formed an intermediate amount of precipitate, as did the FY4 control and the FY4-*met12* $\Delta$  mutant. Finally, the FY4-*met3* $\Delta$ , FY4-*met5* $\Delta$ , and FY4-*met10* $\Delta$  mutants had no discernable precipitate (**Figures 2C-D**), confirming that the SAP is indeed disrupted in these strains as expected given their previously described activities. We saw similar results in a bismuth-containing medium lacking organosulfurs (SD-Met+Glu+Bi; **Figure S6**). Altogether, these observations were consistent with the known roles of the deleted genes in the organosulfur biosynthesis pathway (**Figure 2A**). Therefore, the unexpected growth of FY4-*met15* $\Delta$  and FY4-*met3* $\Delta$  cells could not to be

explained by previous mischaracterizations of the positions of the Met15 and Met3 enzymes in the organosulfur biosynthesis pathway.

To determine whether the surprising growth of FY4-*met15* $\Delta$  and FY4-*met3* $\Delta$  cells in media lacking organosulfurs was dependent on the utilization of inorganic sulfates, we examined the growth of FY4 and the FY4-*met15* $\Delta$  and FY4-*met3* $\Delta$  mutants on plates entirely devoid of both organosulfurs and inorganic sulfates. Applying our automated colony transfer procedure (**Figure 1A**), we pinned cells from rich media to SD-Met+Glu media containing or lacking inorganic sulfates. We observed reduced, but not abolished, growth in the no sulfate condition (SD-Met+Glu without inorganic sulfates) for FY4 and FY4-*met15* $\Delta$ . In contrast, the growth of FY4-*met3* $\Delta$  colonies was unaffected by the presence or absence of inorganic sulfates (**Figure 2E**), arguing against an alternative pathway for the conversion of sulfates to sulfides. We then pinned all three strains from SD-Met+Glu with or without inorganic sulfates to the same medium a second time. Upon so doing, the growth of the FY4-*met15* $\Delta$  strain on the no sulfate medium was essentially abolished, indicating that said growth is dependent on the utilization of inorganic sulfates. The FY4-*met3* $\Delta$  strain failed to show any substantial growth upon a second pinning irrespective of the presence or absence of inorganic sulfates, suggesting that, unlike the stable growth seen in FY4-*met15* $\Delta$  colonies, the growth of FY4-*met3* $\Delta$  colonies observed after a single pinning to organosulfur-free media is not stable under the growth conditions tested here (**Figure 2E**). Thus, the unexpected context-dependent stable growth that we observe in *met15* $\Delta$  cells is specific to the

absence of Met15, is not observed when other key enzymes in the pathway are missing, and is dependent on the utilization of inorganic sulfates.

It is known that *S. cerevisiae* cells experiencing sulfur starvation often arrest rather than die (Petti et al., 2011). We therefore interrogated the extent to which we could restore growth in the above-mentioned strains following successive pinnings to SD-Met+Glu medium lacking sulfates by transferring cells to SD medium containing both methionine and sulfates. Growth was restored in both the FY4-*met15* $\Delta$  and FY4-*met3* $\Delta$  strains that had previously stopped growing, indicating that at least some fraction of the cells were arrested. Furthermore, a dramatic increase in colony size was also observed in FY4, which, surprisingly, had continued to grow on media lacking in both organosulfurs and inorganic sulfates even after five successive pinnings, albeit to a significantly reduced colony size (**Figure 2E**). In this sense, in our automated colony transfer procedure, FY4-*met15* $\Delta$  cells growing in media completely lacking inorganic sulfates display growth behavior similar to that previously observed in conditions of low methionine (Petti *et al.*, 2011); that is, unlike most auxotrophs deprived of a required nutrient, they have a tendency to undergo arrest rather than cell death.

### ***YLL058W* is critical for the growth of organosulfur-starved *met15* $\Delta$ cells**

The highly stable nature of the growth of FY4-*met15* $\Delta$  colonies on organosulfur-free media that we observed (**Figure 1G**) led us to hypothesize that the *S. cerevisiae* genome encoded at least one enzyme, other than Met15, capable of catalyzing *de novo* homocysteine biosynthesis. The protein encoded by the little-studied, uncharacterized

open reading frame (ORF) *YLL058W* stood out as an intriguing candidate for several reasons. First, sequence analyses placed *YLL058W* as a part of the PLP-dependent transferase superfamily, together with Met15 and nine other *S. cerevisiae* genes primarily involved in sulfur metabolism (Wilson et al., 2009). Second, transcription of *YLL058W* is activated by Met4, the master transcriptional activator of the sulfur metabolic network (Lee et al., 2010). Third, a global examination of the expression changes associated with methionine restriction showed that expression of *YLL058W* is significantly upregulated at both the mRNA and protein level upon reduction of methionine levels (Zou et al., 2017). Finally, in *S. cerevisiae*, the *YLL058W* gene is located near the telomere of chromosome 12 within a sizeable cluster of genes that are transcriptionally regulated by Met4, several of which are known to have a direct role in sulfur metabolism (**Figure 3A**) (Lee et al., 2010). It has been noted that this concentration of related genes is reminiscent of a bacterial operon. Therefore, there has been speculation that *YLL058W* may have arisen as a result of horizontal transfer (Lee et al., 2010) - a relatively rare occurrence in yeast.

We thus pursued further investigation of the *YLL058W* ORF, beginning with its evolutionary origins. Besides belonging to the same superfamily as Met15, *YLL058W* has two known close paralogs in the *S. cerevisiae* genome: *STR2*, which encodes an enzyme that converts cysteine into cystathionine (**Figure 2A**), and the uncharacterized ORF *YML082W*, which is a copy of *STR2* generated during the *S. cerevisiae* whole-genome duplication event (Byrne and Wolfe, 2005). We identified bacterial or fungal homologs of *YLL058W*, *STR2*, and *YML082W* using BLASTP and HMMER (Eddy, 2011). We then performed K-means clustering on this collection of homologous

sequences. If *YLL058W* were derived from a recent horizontal transfer event, we would expect it to be more similar to some of its homologs outside *Ascomycota* than to its *Ascomycota* homologs. Instead, we found that all homologs outside *Ascomycota* grouped together along with all budding yeast homologs more distantly related to *S. cerevisiae* than the *Hanseniaspora* genus. We labelled this group of sequences the ancestral class. The homologs found in all descendants of the common ancestor of *Saccharomyces* and *Hanseniaspora* comprised two additional groups, one containing *YLL058W* (*YLL058W* class) and the other containing both *STR2* and *YML082W* (*STR2/YML082W* class) (**Figure S7**). The genes belonging to the *YLL058W* class and the *STR2/YML082W* class appear at approximately the same point in the phylogenetic tree (**Figure 3B**), prior to the whole genome duplication event. Therefore, the most plausible evolutionary scenario is duplication of an ancestral gene into *YLL058W* and the *STR2/YML082W* ancestor, followed by substantial divergence of both copies from the ancestral state, and later by the duplication of the *STR2/YML082W* ancestor. Interestingly, within all species that contain genes of the *YLL058W* class, the *YLL058W* homolog is located near the telomeres among a collection of other sulfur metabolism related genes (**Figure 3A and Table S3**). That this pattern appears to have been preserved since the origin of *YLL058W* in the genomically-unstable near-telomere region is consistent with a strong selective constraint keeping *YLL058W* in proximity to other genes involved in sulfur metabolism.

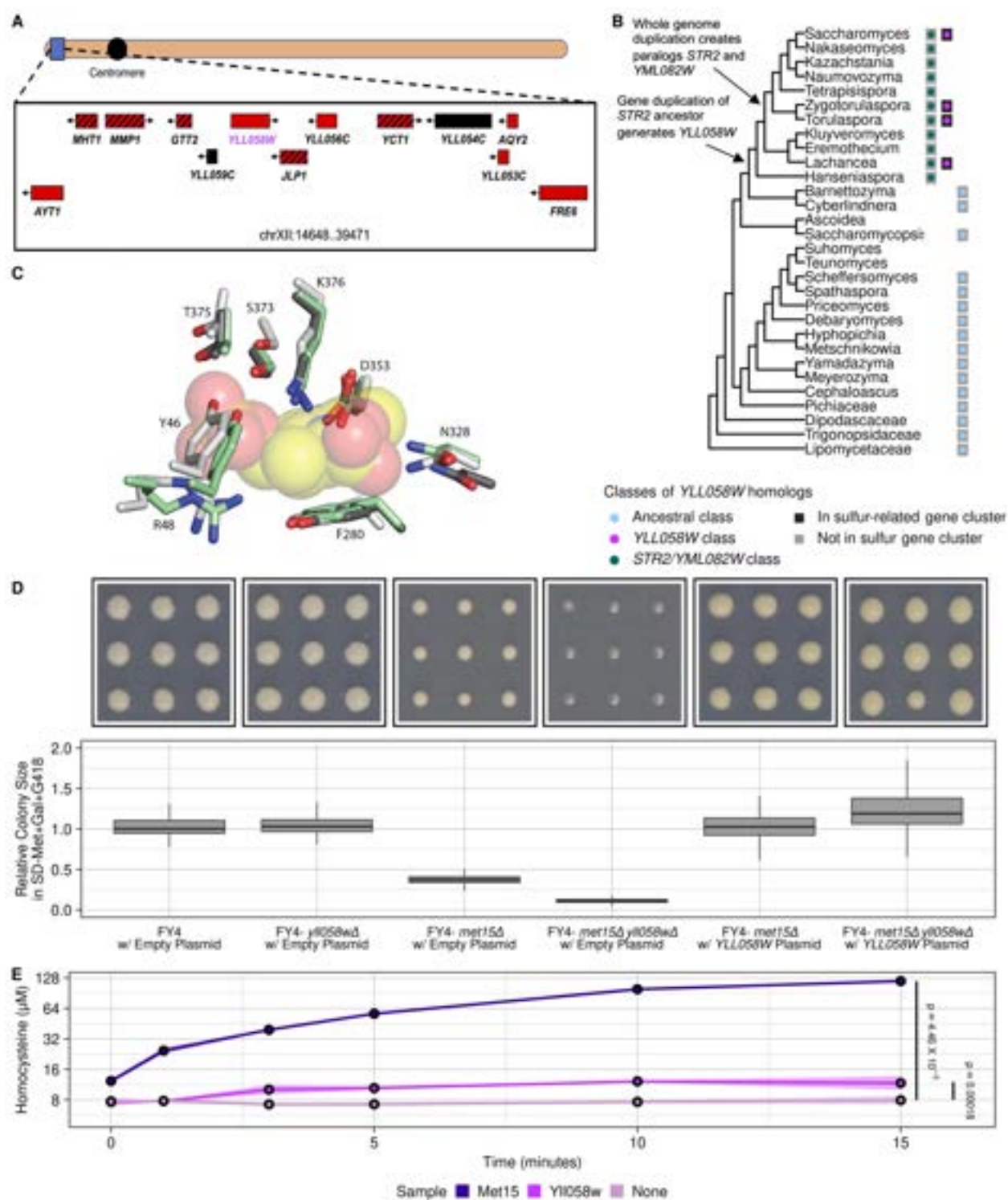


**Figure 3. Yll058w functions as an inefficient homocysteine synthase. A)** Genomic context of *YLL058W* (Stanford University, 2020). In *S. cerevisiae*, *YLL058W* (magenta) is located near a cluster of genes that are transcriptionally activated by Met4 ((Lee *et al.*, 2010); red boxes), several of which have a direct, known role in sulfur metabolism (red boxes with black stripes). Black boxes indicate ORFs that fall into neither category. **B)** Distribution of *YLL058W* clusters across the budding yeast phylogenetic tree,

which follows (Shen et al., 2018). Circles adjacent to each taxon indicate whether *YLL058W* homologs belonging to each of the three classes identified by K-means clustering in the MDS plot (**Figure S7**) are found in the genome of that taxa, while black boxes indicate the presence of a cluster of sulfur-related genes, such as is depicted in Panel A for *S. cerevisiae*. **C**) Yll058w has structural similarity to a homocysteine synthase. Structural overlap of MetY from *Thermatoga maritima* (PDB ID: 7KB1) (pale green), with the predicted structure of Yll058w (white) and Met15 (gray) calculated using AlphaFold. Oxygen atoms are depicted in red, and nitrogen atoms in blue. Just the active site residues are shown for clarity. An O-acetyl-homoserine derivative reaction intermediate captured within the MetY structure (Brewster et al., 2021) is shown in semi-transparent spheres. The active site residues of all three proteins are similar and in similar positions, consistent with Yll058w and Met15 containing homocysteine synthase activity. Numbering corresponds to the Yll058w sequence. **D**) Yll058w is critical for growth in the absence of *MET15*. The indicated strains bearing high-copy ( $2\mu$  ORI) plasmids conferring resistance to G418, and, where indicated, overexpressing *YLL058W*, were grown on SD-Met+Gal medium containing G418 (required for plasmid maintenance). See **Supplementary Material** for details on the plasmid construction. The box plots show colony size (pixel count, y-axis) data for two 384-colony density plates per strain, containing four biological replicates that each have 77 technical replicates (after edges are excluded). The colony sizes at saturation (336 hours) were normalized to FY4 with an empty vector plasmid to obtain a relative colony size. Cropped, representative images of the plates corresponding to the strains tested are shown above. **E**) Yll058w catalyzes homocysteine biosynthesis. An *in vitro* homocysteine biosynthesis assay was carried out using recombinantly expressed, purified *S. cerevisiae* Met15 (violet) or Yll058w (magenta) as the catalyst. All reactions, including control reactions lacking an enzyme (pink), contained O-acetyl-homoserine, hydrogen sulfide, and the coenzyme pyridoxal 5'-phosphate, and were incubated at 30°C. The reactions were conducted in triplicate. A paired Student's t-test combining all replicates and time points for a given sample showed that homocysteine levels were significantly higher than the negative control for both Met15 ( $p=4.46 \times 10^{-5}$ ) and Yll058w ( $p=0.00018$ ). The y-axis is shown on a log<sub>2</sub> scale. See **Experimental Procedures** for details regarding protein purification and buffers used.

The sequence similarity and evolutionary relationship of Yll058w to enzymes involved in sulfur metabolism led us to examine its predicted structure. To do so, we made use of the published crystal structure of MetY, a bacterial O-acetylhomoserine aminocarboxypropyltransferase that catalyzes the biosynthesis of homocysteine from O-acetylhomoserine and bisulfide (Brewster *et al.*, 2021) as well as the predicted structures of Met15 and Yll058w generated by AlphaFold2 (Jumper et al., 2021). The MetY structure captured a reaction intermediate, allowing for a precise determination of active site residues. The predicted 3D structures of both Met15 and Yll058w are highly similar to the experimentally determined structure of MetY within the active site (**Figure 3C**), including the catalytic lysine. One difference is position 280 in the Yll058w sequence, which is a phenylalanine in Yll058w but a tyrosine in both Met15 and MetY. Another difference in the overall fold is that MetY and Met15 function as homotetramers

(Brewster *et al.*, 2021; Yamagata, 1976), with multimerization domains allowing the distinct monomers to come together to complete the active site. In contrast, YII058w lacks such a multimerization domain and is predicted to be monomeric. However, it contains an approximately 180 amino acid region before the catalytic domain that has no homology to MetY or Met15. This region folds back onto the core of the protein, supplying the missing amino acids to the active site (YII058w tyrosine 46 and arginine 48). Altogether, these comparative structural analyses suggest that a YII058w monomer may be capable of carrying out catalysis similar to that of the MetY and Met15 tetramers.

We thus sought to determine whether the putative YII058w enzyme is necessary and sufficient to support growth of *met15Δ* cells in the absence of exogenous organosulfurs using genetic approaches. We made a CRISPR deletion of *YLL058W* in the FY4 background in the same fashion as the mutants we had previously examined and also utilized CRISPR to make a *met15ΔyII058wΔ* double mutant in the FY4 background. We also constructed high copy-number (2 $\mu$  ori) plasmids expressing *YLL058W* from a highly active, constitutive promoter (GPD). Consistent with the fact that deletion of *YLL058W* in isolation has not been previously associated with a specific phenotype, the FY4-*yII058wΔ* single mutant resulted in only a very modest growth defect on SD-Met+Glu (effect size = 0.054, p-value > 0.05 [Kruskal-Wallis test]) (**Figure S8A**), and when grown on bismuth-containing medium displayed an intermediate level of precipitate (**Figure S8B-C**) comparable to FY4-*met12Δ* and the FY4 parent (**Figures 2B-D and S6A-B**). Strikingly however, the FY4-*met15ΔyII058wΔ* double mutant showed little to no growth in the absence of exogenous organosulfurs (**Figure 3D**), indicating a

synthetic lethal interaction between *MET15* and *YLL058W*. To verify that this synthetic lethal interaction was due to the loss of the *YLL058W* gene product, we compared the growth of FY4-*met15* $\Delta$  and FY4-*met15* $\Delta$ *yll058w* $\Delta$  strains carrying an empty vector plasmid to the same strains carrying plasmids overexpressing *YLL058W*.

Overexpression of *YLL058W* in the FY4-*met15* $\Delta$ *yll058w* $\Delta$  background resulted in a large, statistically significant increase in growth (effect size= 9.478, p-value < 0.001 [Kruskal-Wallis test]). Overexpression of *YLL058W* also significantly enhanced the growth of the FY4-*met15* $\Delta$  single mutant (effect size= 1.703, p-value < 0.001 [Kruskal-Wallis test]) (**Figure 3D**). This genetic evidence strongly suggests that the unexpected growth of *met15* $\Delta$  colonies in the absence of exogenous organosulfurs is mediated by the putative enzyme encoded by *YLL058W*.

To directly examine the ability of Yll058w to catalyze homocysteine biosynthesis, we purified recombinant protein from *E. coli*, along with Met15 as a positive control, and carried out *in vitro* reactions using a modified version of a validated assay (Chen *et al.*, 2018) (**Experimental Procedures**). This assay uses the canonical O-acetyl-homoserine and hydrogen sulfide as substrates and includes in the reaction mixture pyridoxal 5'-phosphate (PLP), a cofactor known to be critical for Met15 activity. We found that Yll058w was able to catalyze homocysteine production significantly above background (determined by measuring homocysteine levels in a “no enzyme” control reaction), albeit much less efficiently than the canonical homocysteine synthase Met15, with the Met15 reactions yielding ~9.9 times as much homocysteine at the 15-minute time point (**Figure 3E**).

We sought to investigate whether such inefficient *de novo* homocysteine biosynthesis would be sufficient to support growth in the absence of Met15 using metabolic modeling. To do so, we adapted an enzyme-constrained version of Yeast8, the current consensus genome-scale metabolic model in *S. cerevisiae* (Lu et al., 2019) (see **Experimental Procedures** for details). We first removed all of the hypothetical YII058w-“consuming” reactions (the steady-state model treats enzymes as metabolites that are “consumed” while engaged in catalysis) and replaced them with our observed *in vitro* reaction. This had little effect on the flux of the biomass equation, a proxy for growth in this *in silico* system. We next removed *MET15* from the model and evaluated the flux through the biomass equation at a broad range of arbitrarily assigned catalytic efficiencies ( $K_{cat}$ ) for YII058w. We found that an appreciable reduction in biomass occurred only when YII058w was assigned a catalytic efficiency ~100x lesser than that of the efficiency assigned to Met15 in the consensus model (**Figure S9**). These simulations, together with our structural (**Figure 3C**), *in vivo* (**Figure 3D**), and biochemical (**Figure 3E**) findings, demonstrate that it is plausible that YII058w enables cells to utilize inorganic sulfates to grow in the absence of *MET15*.

### **Removal of H<sub>2</sub>S enhances the growth of *met15Δ* cells in organosulfur-free media**

Our observations (**Figure 1**) show that the stable growth of *met15Δ* cells in the absence of exogenous organosulfurs highly depends on the manner in which cells are propagated and on the carbon source that they are able to utilize. Specifically, we see that *met15Δ* cells do indeed display auxotrophic-like phenotypes when propagated using the type of conventional methods that were almost exclusively in use at the time

of the gene's initial characterization, such as liquid cultures in flasks or thick patches on Petri dishes, and that these same cells also fail to grow when EtOH is used as a carbon source. It may be that *met15Δ* cells may fail to grow in these contexts not due to organosulfur starvation *per se*, but to some downstream cause brought about by the loss of Met15 activity. One such cause may be the large excess of H<sub>2</sub>S present in *met15Δ* cells that we (**Figures 2C-D and S6A-B**) and others (Brachmann *et al.*, 1998; Cost and Boeke, 1996; Ono *et al.*, 1991) have observed. This accumulation of H<sub>2</sub>S is expected in *met15Δ* cells since the reaction catalyzed by Met15 is one of the major sulfide-consuming reactions in the cell. Although some amount of H<sub>2</sub>S is required for cell growth, at high levels it is toxic via several mechanisms, including through inhibition of the reaction catalyzed by cytochrome c oxidase, a critical step in mitochondrial respiration (Blackstone *et al.*, 2005). We thus hypothesized that the growth defect of *met15Δ* cells in our automated colony transfer assay, and their auxotrophic behavior in other contexts, might be partly due to toxic levels of H<sub>2</sub>S.

To investigate this hypothesis, we examined the growth of FY4 and FY4-*met15Δ* cells in liquid SD-Met+Glu medium with or without the H<sub>2</sub>S chelator ferric (Fe)-EDTA (**Figure 4A**). This chelator binds free sulfides that exit the cell by diffusion, thereby alleviating toxicity (Gaensly *et al.*, 2014; Philip and Brooks, 1974). Each culture was grown in triplicate, in individual flasks, and the experiment was repeated twice. In the presence of the chelator, the growth of FY4 cells was modestly enhanced, and we observed a striking increase in the growth of FY4-*met15Δ* cells (p-value = 0.01 [Student's t-test]; **Figure 4B**, top right panel). To rule out spontaneous mutations as the reason for this increase in growth, we then repassaged each sample in SD-Met+Glu medium lacking

chelator (**Figure 4A**). Interestingly, the FY4 cultures that had previously been propagated in the presence of chelator saturated at a higher OD<sub>600</sub> than those that had not (p-value = 0.0012 [Student's t-test]; **Figure 4B**, bottom left panel). In contrast, the FY4-*met15*Δ samples that were repassaged showed little to no growth (**Figure 4B**, bottom right panel), consistent with the auxotrophic-like phenotype of *met15*Δ cells propagated in this manner (**Figure 1E**). We then placed cells from both the original and the repassaged cultures on five plates of solid media with different composition (YPDA, SD-Met+Glu, SC-Met-Cys+Glu, SC-Met-Cys+Glu+Fe-EDTA, and BiGGY) in large drops and patches (as depicted in **Figure 4A**) to determine if the failure of thick patches of *met15*Δ cells to grow that we observed previously (**Figures 1F and S2**) was affected by the prior passage in liquid media containing chelator. The FY4-*met15*Δ cells failed to grow on SD-Met+Glu and SC-Met-Cys+Glu in drops or patches, irrespective of their previous exposure to the chelator (**Figure 4C**). These results demonstrate that the growth of FY4-*met15*Δ cells in the presence of chelator is not facilitated by heritable mutations and confirms our previous observations that *met15*Δ cells grown in patches behave as auxotrophs. However, upon adding Fe-EDTA to the solid medium, this lack of growth was partially rescued (**Figure 4C**). FY4-*met15*Δ grown on BiGGY retained their dark brown color (**Figure 4C**), indicating that the cells were still producing an excess of H<sub>2</sub>S in the absence of the chelator. Thus, the growth defect (in some settings) and auxotrophic behavior (in other settings) of *met15*Δ cells grown without organosulfurs is at least partially attributable to H<sub>2</sub>S toxicity.

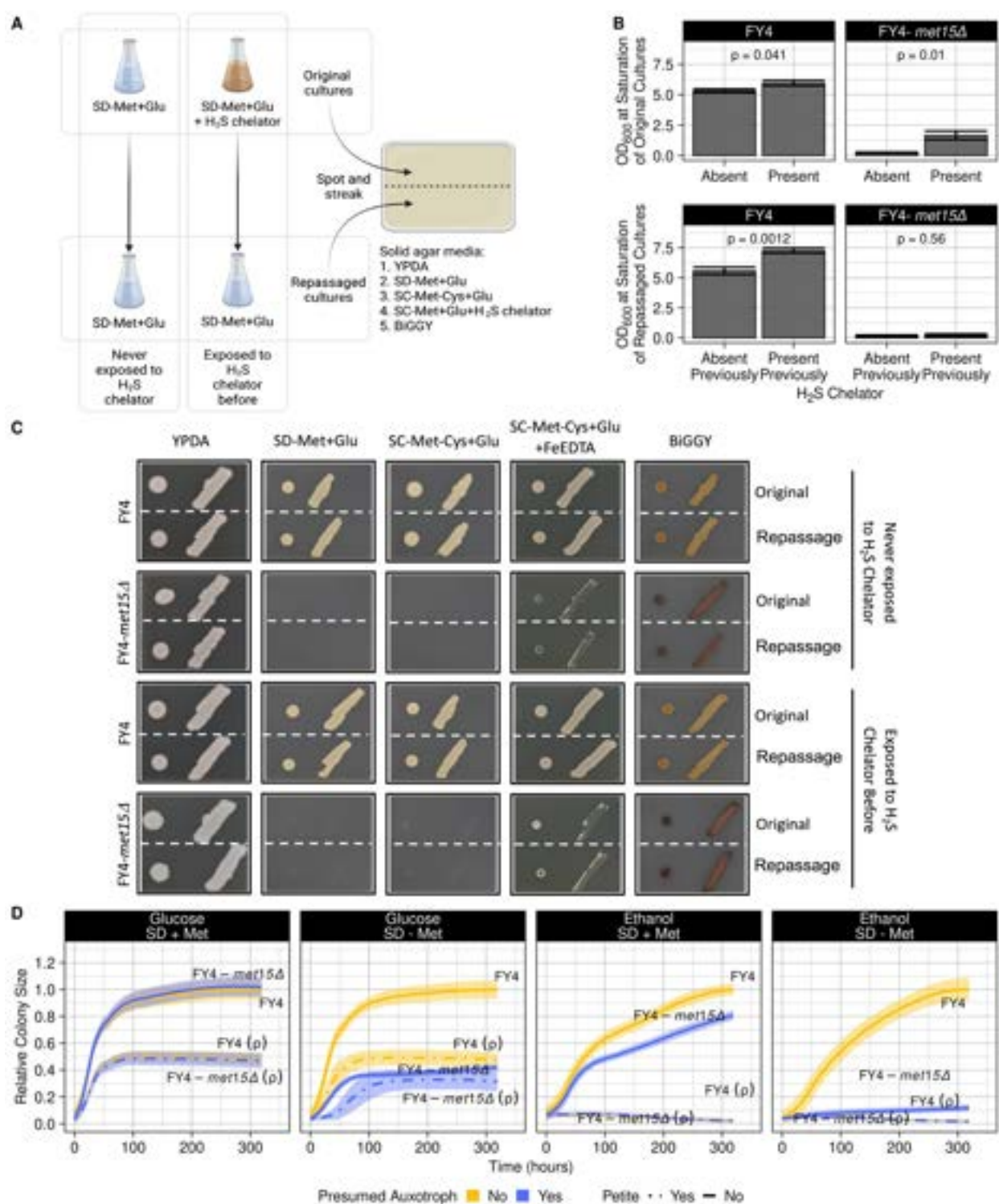


**Figure 4. Chelation of H<sub>2</sub>S facilitates the growth of *met15Δ* cells in the absence of exogenous organosulfurs.** **A)** Experimental setup. Strains were grown in individual Erlenmeyer flasks in either SD-Met+Glu or SD-Met+Glu+Fe-EDTA liquid media. The optical density at 600nm (OD<sub>600</sub>) was measured regularly on a spectrophotometer until saturation was reached for all cultures. These cultures were then repassaged in SD-Met+Glu media (bottom two flasks, repassaged cultures) and again grown to saturation OD<sub>600</sub> values for original and repassaged cultures are shown in Panel B. In this experimental setup, there

were cells that were never exposed to the H<sub>2</sub>S chelator (left column) and those that were only exposed in the original cultures before (right column). Cells from each culture were then spotted and struck to the indicated solid media (Panel C). Each culture was grown in triplicate, in individual flasks, and the experiment was repeated twice. **B)** The H<sub>2</sub>S chelator Fe-EDTA partially rescues the growth of *met15Δ* cells grown in liquid media. OD<sub>600</sub> values of the cultures depicted in Panel A after ~51 hours of growth with or without chelator at 30°C (top), and after the same cells were diluted to the same inoculation density and grown again in SD-Met+Glu without chelator for ~51 hours at 30°C (bottom), are shown. The p-values shown at the top of the subpanels were calculated with a paired Student's t-test using the OD<sub>600</sub> values at saturation. Presence of the chelator increases growth of FY4-*met15Δ* cells (top right). Removal of the chelator causes the reversion of *met15Δ* cells to an auxotrophic growth phenotype in liquid (bottom right). The individual values for each replicate, from two independent experiments, are shown in **Table S4**; outlier FY4-*met15Δ* cultures that showed unexpected growth in SD-Met+Glu were excluded from the data presented here and indicated in green text in the table. **C)** Chelation of H<sub>2</sub>S partially rescues the growth of FY4-*met15Δ* cells grown in spots or streaks. Ten μl of each culture, were spotted and struck to the indicated solid agar media and grown at 30°C for 192 hours (see **Panel A** and **Experimental Procedures**); the images shown are representative. **D)** A growth defect of *met15Δ* cells grown with ethanol is seen in the presence and absence of organosulfurs in the media. Growth curves of FY4 and the FY4-*met15Δ* mutant, along with their respective petite ( $\rho^-$ ) derivatives, pinned on SD media containing or lacking methionine and utilizing either glucose or ethanol as the sole carbon source are shown. For each condition, the pinning procedure and plate construction were as described in **Figure 1A** and **Experimental Procedures**. The colony size (pixel count) data used to make the growth curves comes from two 384-colony density plates per strain, containing four biological replicates that each have 77 technical replicates (after edge colonies are excluded). All colony sizes were normalized to the median colony size of FY4 at the final time point. The mean relative colony size is represented by the solid or dashed lines, and the shaded region represents the standard error. **Table S5** contains the Kruskal-Wallis Test results comparing the growth of a particular strain as estimated by Area Under the Curve in the presence or absence of methionine in media containing either glucose or ethanol as the carbon source.

Given that H<sub>2</sub>S toxicity involves mitochondrial impairment, we further investigated whether the context-dependent growth phenotypes of *met15Δ* cells might be caused by H<sub>2</sub>S induced mitochondrial damage. In agreement with this hypothesis, we have observed that *met15Δ* cells failed to grow when EtOH was used as a carbon source (**Figures 1C** and **S4B**). Strains with either damaged or absent mitochondrial genomes, or mutations to certain nuclear genes that result in dysfunctional mitochondria, display what is known as the petite phenotype, and are incapable of efficient respiration and cannot utilize non-fermentable carbon sources such as EtOH (Ferguson and von Borstel, 1992). We constructed petite ( $\rho^-$ ) derivatives of FY4 and FY4-*met15Δ* (**Experimental Procedures**). Using the pipeline described in **Figure 1A**, we transferred these strains and their respective non-petite parental strains to media containing or

lacking methionine, and with either glucose or EtOH as the carbon source (**Figure 4D**). Non-petite FY4-*met15*Δ cells grew poorly relative to their *MET15*<sup>+</sup> counterparts when EtOH was used as the carbon source in SD medium containing methionine. Although distinguishable from the petite phenotype, this growth defect is consistent with possible mitochondrial dysfunction in *met15*Δ cells. Furthermore, *met15*Δ ρ<sup>-</sup> strains grew on SD-Met+Glu almost as well as their non-petite parental strains, suggesting that fully functional mitochondria are not required for the unexpected growth of *met15*Δ cells that we observe in this context. Altogether, our observations support a model according to which *met15*Δ cells experience chronic H<sub>2</sub>S toxicity leading to mitochondrial impairment but can still synthesize enough homocysteine to support growth (**Figure 5**).

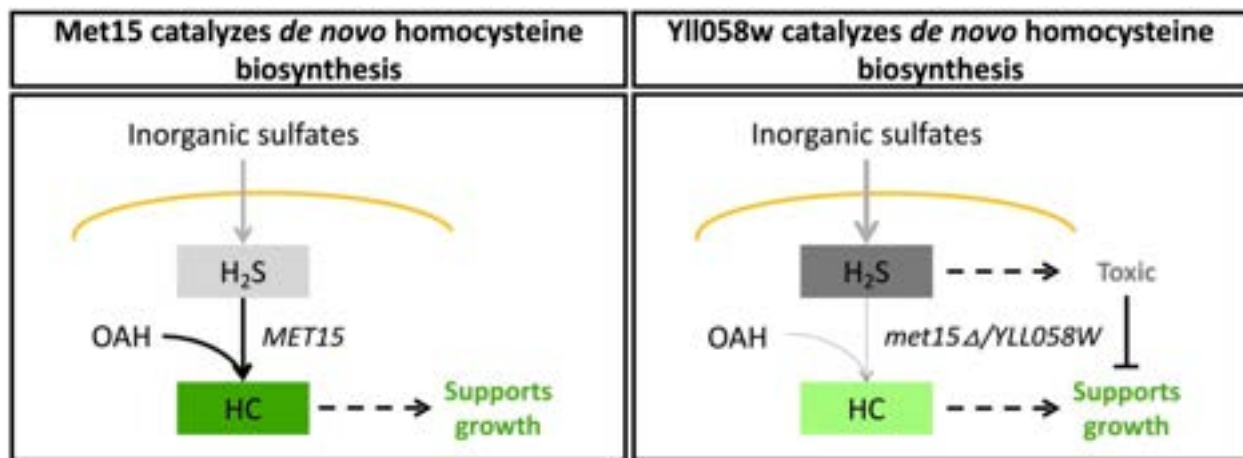


**Figure 5. H<sub>2</sub>S toxicity inhibits growth when Yll058w catalyzes *de novo* homocysteine biosynthesis.**

This model represents what we hypothesize happens when cells are grown on media lacking organosulfurs. Extracellular inorganic sulfates are imported through the cell membrane (yellow line) and reduced to H<sub>2</sub>S. When Met15 is present (left panel), cells can efficiently convert H<sub>2</sub>S and O-acetylhomoserine (OAH) into homocysteine, leading to a moderate amount of H<sub>2</sub>S (light gray) and an adequate amount of homocysteine to support growth (HC; dark green). When Met15 is absent, cells are forced to generate homocysteine through the comparatively inefficient Yll058w enzyme (right panel). The resulting lower amount of homocysteine (light green) is sufficient to support growth in some contexts, but the high amount of H<sub>2</sub>S that accumulates (dark gray) can become toxic and lead to cell death or arrest, and the appearance of auxotrophy, in other contexts.

## DISCUSSION

There has been a renewed interest of late in sulfur metabolism generally and more specifically in methionine metabolism, due to, among other things, the fact that methionine restriction plays a role in increasing longevity in a broad range of organisms (Green et al., 2021), and may also serve as a possible therapeutic intervention in the treatment of certain cancers (Endicott et al., 2021). There has also been a recently appreciated connection between cysteine and mitochondrial function (Hughes et al., 2020). Prokaryotes, fungi, and plants are uniquely capable of synthesizing organosulfurs from inorganic sulfur compounds, and yet many of the critical enzymes involved in this process remain understudied. This applies to the *S.*

*cerevisiae* homocysteine synthase encoded by the *MET15* gene, which despite its critical role in connecting the sulfate assimilation pathway to *de novo* organosulfur biosynthesis, had primarily been studied and exploited as an auxotrophic marker and tool for genetic manipulation. In this work we show that, contrary to longstanding assumptions, organosulfur auxotrophy in a *met15Δ* background is context-dependent.

Our analyses demonstrate that the *S. cerevisiae* genome and those of several closely related species encodes another enzyme, the previously uncharacterized YII058w, that can catalyze the same reaction as Met15, albeit less efficiently. Given its evolutionary conservation, YII058w may well have other biological activities that are not investigated here. We show that the homocysteine synthase activity we uncovered for YII058w can compensate for the loss of *MET15* and enable growth of *met15Δ* cells in the absence of exogenous organosulfurs when cells are propagated using automated colony transfer or

grown in the presence of an H<sub>2</sub>S chelator. Altogether, our results strongly suggest that H<sub>2</sub>S toxicity is at least partially responsible for the arrest and/or death that occurs in *met15Δ* cells grown using conventional techniques, leading to auxotrophic-like growth phenotypes (**Figure 5**).

H<sub>2</sub>S levels are extremely high when *met15Δ* cells are growing without exogenous organosulfurs (**Figure S6**), due in part to the well-documented strong upregulation of the SAP upon organosulfur starvation (Hansen and Johannesen, 2000; Zou *et al.*, 2017). Our experiments suggest that these high levels of H<sub>2</sub>S may impair mitochondrial function to such an extent that *met15Δ* cells die or arrest when deprived of external organosulfurs. The precise molecular mechanisms at play may be dissected in future genome-scale investigations of suppressor and synthetic lethal mutations, similar to how a recent study dissected the mechanisms underlying the growth defect associated with petites phenotypes (Vowinckel *et al.*, 2021). Based on the data we generated in this study, we hypothesize that *met15Δ* cells grow when propagated with automated colony transfer because the excess sulfide is likely eliminated through diffusion between the evenly spaced small colonies. In the context of thick patches of cells, where we see a lack of growth consistent with auxotrophy, any sulfides secreted by cells are probably affecting neighboring cells, creating group-level toxicity and thereby limiting growth. Similarly, we hypothesize that H<sub>2</sub>S toxicity is high in liquid cultures because they are typically performed in a semi-sealed environment, limiting the amount of gas exchange that can occur.

It is of note that even our prototrophic FY4 control displayed enhanced growth in liquid media when cells were previously exposed to an H<sub>2</sub>S chelator (**Figure 4B**). These findings suggest that 1) even wild-type cells suffer some degree of H<sub>2</sub>S-induced stress when grown in organosulfur-free media, and 2) that removal of excess H<sub>2</sub>S allows the cells to adapt to this stress, likely at the level of gene expression or epigenetics, such that they grow better upon repassage in this same media even in the absence of a chelator. This finding may have implications for anyone seeking to maximize cellular growth in media lacking or containing low amounts of organosulfurs, whether in an industrial or a research setting.

In summary, we have demonstrated for the first time an *in vivo* and *in vitro* function for the *S. cerevisiae* *YLL058W* gene, showing that it encodes an inefficient homocysteine synthase. This activity facilitates robust and stable growth of *met15Δ* cells propagated using automated colony transfer in organosulfur-free media, contrary to the assumption that such cells are strict organosulfur auxotrophs. Our demonstration that *S. cerevisiae* can display stable growth in organosulfur-free media despite very low levels of *de novo* homocysteine biosynthesis has implications for a range of studies, particularly those involving methionine restriction, and may represent a novel tool for the study of organosulfur starvation more broadly.

## MATERIALS AND METHODS

### Yeast strains

The well-characterized S288C-derived *Saccharomyces cerevisiae* strains FY4, BY4741 and BY4742 were used throughout this work (Brachmann *et al.*, 1998; Winston *et al.*, 1995).

### Construction of strains with CRISPR/Cas9 deletions

All other strains (**Table S6**) were derived by CRISPR/Cas9 based scarless whole-ORF deletions of genes from the prototrophic strain, FY4. CRISPR deletion mutants were made with co-transformation of 5 $\mu$ g of repair fragment and 1 $\mu$ g of plasmid expressing cas9 (Addgene 60847) (Ryan *et al.*, 2014) with the respective sgRNA (DiCarlo *et al.*, 2013). Identification of PAM sites and sgRNA selection were chosen using Benchling (<https://www.benchling.com/>). Transformed cells were plated on YPDA+G418 and colonies were PCR genotyped to select those with the correct gene deletion. The positive clones were then grown on YPDA to induce the loss of the cas9- and sgRNA-containing plasmids. The sgRNA and repair fragment sequences are given in **Table S8**.

### Plasmid construction

The overexpression plasmids used in **Figure 3D** were made by replacing the Leu2 gene by KanMx cassette into the destination plasmid pAG425GPD-ccdB (Alberti, 2007). This plasmid was used as an empty vector plasmid (pARC0112, **Table S7**) while an LR recombination (Gateway LR Clonase II Enzyme Mix, ThermoFisher) of this same

plasmid with an entry clone containing the ORF *YLL058W* was used to produce the plasmid overexpressing *YLL058W* (pARC0172, **Table S7**).

The plasmids pARC0002 and pARC0002-*MET15* (**Table S7**) used in **Figure S1** are described on Butcher et.al., 2006 and Douglas et.al., 2012. pARC0002 was obtained from Dana-Farber/Harvard Cancer Center, while the plasmid overexpressing *MET15* was extracted with Zymoprep Yeast Plasmid Miniprep I (Zymo Research) from a strain carrying the plasmid, from the BarFLEX overexpression collection (Douglas et.al., 2012).

Plasmids pARC0190 and pARC0191 (**Table S7**) were made by amplification of *MET15* and *YLL058W* coding sequences, respectively, from *S. cerevisiae* genomic DNA, and cloned into a pET28a-derived vector expressing an N-terminal, cleavable 10XHis-Ruby tag (Kredel et.al., 2009).

### **Construction of strains carrying overexpression plasmids**

Strains carrying plasmids for overexpression experiments were made with the LiAc/PEG/ssDNA protocol (Dunham, 2015) using 500ng of each plasmid and selected on the corresponding selective media.

### **Construction of petite strains**

Petite derivatives of FY4 and FY4-*met15*Δ were made using a slightly modified version of the standard LiAc/PEG/ssDNA yeast transformation protocol (Dunham, 2015), with shorter incubation times and without a DNA template, followed by replica plating on YPDA and YP-Glycerol plates to identify the petites.

## **Strain stock plates**

Stock plates were constructed for each strain by selecting four independent colonies from streakouts, used to inoculate individual liquid YPDA medium, and grown overnight at 30°C. These cultures were considered biological replicates. The cultures were then used to create 384-well glycerol stocks (15% glycerol) for each strain, with each biological replicate occupying one-fourth of the wells. The stocks were stored at -80°C before use. The benchtop RoToR HDA robotic plate handler (Singer Instruments Co Ltd, Roadwater, UK) was used for plate-to-plate cell transfer (see **Table S1** for a description of the settings used).

## **Growth Media**

The recipes for all the various growth media used in this study are given in **Table S9**.

## **Strain Crossing**

The cross depicted in **Figure S2** was carried out by standard techniques. Briefly, the BY4741 and BY4742 deletion collection parent strains (**Table S6**) were mated on YPDA solid medium and incubated at room temperature (RT) for ~6 hours, and then struck to select for colonies formed from single diploids on solid SD+His+Leu+Ura medium. After incubation at 30°C for ~2 days on the diploid selection medium, colonies were patched to “GNA” plates (**Table S9**) and incubated at 30°C for ~2 days. These plates were then replica plated to “sporulation (SPO)” medium (**Table S9**) containing histidine, lysine, uracil, and leucine, and incubated at RT for ~11 days. Four-spore tetrads were selected

and dissected using standard techniques and initially grown on YPDA. Individual spores were then patched to mini petri dishes as shown in **Figure S2**.

### **Automated Colony Transfer**

Using the benchtop RoToR HDA robotic plate handler (Singer Instruments Co Ltd, Roadwater, UK) strains were transferred from glycerol stocks to solid rich medium plates (YPDA, **see Supplementary Material**) and incubated at 30°C for 72 hours. Each of these plates were copied to two YPDA plates, which represented the two technical replicates of plates per strain, and again incubated at 30°C for 48 hours. This step reduces the variability in colony size that is introduced when cells are pinned from glycerol stocks. Finally, these plates were ‘one-to-many’ copied onto respective solid ‘condition’ media plates (**see Supplementary Material**) depending on the experiment. The plates were incubated at 30°C until the colonies reached saturation. This protocol is shown in **Figure 1A**. Saturation in the solid condition media was determined as the point at which the colonies would touch each other if the plates were incubated for any longer or at the point at which they visually appeared to have stopped growing. This experimental protocol carried out at least twice per experiment to control for batch effect.

### **Colony size estimation**

Serial imaging of the plates was done either manually or using splmager Automated Imaging System (S & P Robotics Inc., Ontario, Canada). Manual imaging was conducted using a custom-made lightbox with an overhead camera mount using a commercially available SLR camera (18Mpixel Rebel T6, Canon USA Inc., Melville, NY,

USA). The plates were imaged at regular intervals beginning right after pinning until the colonies reached saturation. The images were analyzed in bulk using a custom script made using functions from the MATLAB Colony Analyzer Toolkit (Bean et al., 2014) to provide colony size estimations

([https://github.com/sauriiin/lid\\_personal/blob/master/justanalyze.m](https://github.com/sauriiin/lid_personal/blob/master/justanalyze.m)). The output files containing colony size information along with the images is available at <https://bit.ly/3pOe6aT>.

### **Relative fitness measurement**

A spatially cognizant colony size database was built using the colony size estimates per the LI Detector framework for high-throughput colony-based screening analysis (Parikh et al., 2021). For all experiments, first, the outermost border colonies were removed from the dataset because these usually tend to grow more due to excess access to nutrients. Outlier colony size values per experiment per technical replicate per time point per plate per biological replicate were removed using two median adjusted deviations. At this stage there would be a maximum of 77 colony size observations per strain per time point per plate per biological replicate. The median colony size per time point of the prototrophic strain, FY4, was used to calculate relative colony size of every colony per strain per time point. At saturation, the relative colony size distribution per strain is determined by the median relative colony sizes per plate per biological replicate. This relative colony size distribution is compared amongst strains using the non-parametric Kruskal-Wallis Test to determine significant changes in fitness. Effect

size values are calculated as the difference in median colony sizes divided by the median colony size of the strain being used as reference in the comparison.

Additionally for **Figure 4D and Table S5**, growth curve analysis was done with the *growthcurver* (Sprouffske and Wagner, 2016) package in R (Team, 2021), using the time series colony size data per colony per strain per technical replicate per biological replicate. This time series data was first converted into an equally spaced time series using a second degree locally weighed scatterplot smoothing (loess) function to generate 100 equally spaced data points. This was then fed into the '*SummarizeGrowthByPlate()*' function of the *growthcurver* package (Sprouffske and Wagner, 2016) to make estimates of the area under the curve (AUC) per colony per strain in the experiment. AUC summarizes a growth curve by integrating the contributions of the initial population size, growth rate, and carrying capacity into a single value, making it a more robust estimation of growth-curve-based 'fitness.' Relative area under the curve, effect sizes and significant changes were estimated the same way as the colony size data described above. The AUCs from the data in **Figure 4D** were used to calculate the statistics in **Table S5**.

## **Mass spectrometry analysis of media by semi-targeted high-resolution LC-HRMS**

### **Sample preparation**

Metabolic quenching and polar metabolite pool extraction was performed by adding 400 $\mu$ L ice cold methanol to 100 $\mu$ L of sample. Deuterated ( $D_3$ )-creatinine and ( $D_3$ )-alanine, ( $D_4$ )-taurine and ( $D_3$ )-lactate (Sigma-Aldrich) was added to the sample lysates

as an internal standard for a final concentration of 10 $\mu$ M. Samples were vortexed, and then homogenized using a 25°C water bath sonicator for 5 minutes. The supernatant was then cleared of protein by centrifugation at 16,000xg. Two  $\mu$ L of cleared supernatant was subjected to online LC-MS analysis.

### **LC-HRMS Method**

Analyses were performed by untargeted LC-HRMS. Briefly, Samples were injected via a Thermo Vanquish UHPLC and separated over a reversed phase Thermo HyperCarb porous graphite column (2.1 $\times$ 100mm, 3 $\mu$ m particle size) maintained at 55°C. For the 20 minute LC gradient, the mobile phase consisted of the following: solvent A (water / 0.1% formic acid) and solvent B (ACN / 0.1% formic acid). The gradient was the following: 0-1min 1% B, increase to 15%B over 5 minutes, continue increasing to 98%B over 5 minutes, hold at 98%B for five minutes, reequilibrate at 1%B for five minutes. The Thermo IDX tribrid mass spectrometer was operated in positive ion mode, scanning in ddMS<sup>2</sup> mode (2  $\mu$ scans) from 70 to 800 m/z at 120,000 resolution with an AGC target of 2e5 for full scan, 2e4 for ms<sup>2</sup> scans using HCD fragmentation at stepped 15,35,50 collision energies. Source ionization setting was 3.0kV spray voltage for positive mode. Source gas parameters were 35 sheath gas, 12 auxiliary gas at 320°C, and 8 sweep gas. Calibration was performed prior to analysis using the Pierce<sup>TM</sup> FlexMix Ion Calibration Solutions (Thermo Fisher Scientific). Integrated peak areas were then extracted manually using Quan Browser (Thermo Fisher Xcalibur ver. 2.7) (Metabolomics & Lipidomics Core, University of Pittsburgh Health Sciences Core Research Facilities).

## Evolutionary origins of *YLL058W*

Genome sequences of 332 budding yeasts were taken from a published dataset (Shen *et al.*, 2018). Each genome was scanned for ORFs (consisting of the sequence between an ATG start codon and a stop codon in the same frame) larger than 300 bp. We then used BLASTP on the predicted protein products of these ORFs to identify the strongest match among *S. cerevisiae* annotated genes. BLASTP was run with default settings and a  $10^{-4}$  e-value cutoff. All ORFs for which the best match (i.e., the lowest BLASTP e-value) was either the *S. cerevisiae* *YLL058W* sequence or the sequence of one of its two *S. cerevisiae* homologs (*STR2* and *YML082W*) were retained. For each ortholog identified, we also noted the best *S. cerevisiae* matches for the 5 nearest ORFs in each direction that had a match. To supplement this list with orthologs from more distant species, we submitted the *S. cerevisiae* *YLL058W* sequence to the HMMER homology search tool (Eddy, 2011). From these results, we selected the strongest matching sequences (lowest e-values) from a variety of bacterial and fungal taxa outside of the *Ascomycota* phylum (four bacterial and nine fungal outgroups). The full list of *YLL058W* homologs and their sequences is given in **Supplementary File 1**.

We next constructed a multiple alignment of all homologs using the MUSCLE aligner (Madeira *et al.*, 2019). We used the R package *bio2mds* to perform K-means clustering on the sequence alignment and to visualize the results using multidimensional scaling. To investigate the phylogenetic distribution of each cluster within budding yeasts, we used the phylogeny generated by the same study of budding yeasts that formed the foundation of our sequence dataset (Shen *et al.*, 2018).

## **Purification of recombinantly expressed proteins**

Both Met15 or YII058w were expressed as fusion proteins with an N-terminal His<sub>10</sub>-mRuby2 tag which can be removed by cleavage with TEV protease. Fusion proteins were expressed in the BL21 (DE3) RIPL CodonPlus *E. coli* strain (Stratagene). Cells were grown at room temperature in 2L of standard LB media containing kanamycin and chloramphenicol to an OD<sub>600</sub> of ~0.6, induced with 0.5mM IPTG, and grown for eight additional hours at room temperature post-induction. Purification of both proteins was performed essentially as described previously (Van Oss et al., 2016). Briefly, both proteins were purified by two rounds (pre- and post-cleavage with TEV protease) of nickel affinity chromatography followed by ion exchange chromatography. Met15 was further purified by size exclusion chromatography. The final purified fractions that were used in the *in vitro* homocysteine assay are shown in **Figure S10**.

## ***in vitro* homocysteine assay**

*in vitro* homocysteine biosynthesis was carried out largely as described previously (Chen *et al.*, 2018). Aliquots of Met15 and YII058w, purified as described above, were dialyzed into a final storage buffer of 20 mM Tris-Cl pH 8.0, 500 mM NaCl, 20 mM Imidazole, 0.2mM pyridoxal 5'-phosphate (PLP), and 10% glycerol, snap frozen in liquid N<sub>2</sub>, and stored at -80°C. Aliquots were thawed on ice, and the enzymes were diluted in the storage buffer to a concentration of 60nM and preincubated at room temperature for 10 minutes. The enzyme solution was then mixed with diluted 10x, giving a final enzyme concentration of 6nM, with a reaction mixture containing 50 mM Potassium phosphate buffer (pH 7.8), 1.0 mM EDTA pH 8.0, 15.0 mM O-acetyl-L-homoserine, 5.0 mM NaHS,

and 0.6 mM PLP. The reaction components were then mixed by gentle pipetting and incubated at 30°C. Each reaction was performed in triplicate. Samples were removed at 6 timepoints (0, 1, 3, 5, 10, and 15 minutes), and the reactions were stopped by adding 1.0M HCl at a ratio of 10mL for every 100mL of sample, then snap frozen with liquid N<sub>2</sub>. In the same buffer as the reaction mixture but without any enzyme or substrate (but with acid added), we also generated a homocysteine standard curve with seven serial 1:5 dilutions ranging from 15mM to 0.00096mM, as well as a 0mM “blank” sample.

Ten µL of each enzyme reaction were extracted and derivatized with N-ethylmaleamide (NEM; Alfa Aesar, Cat# 40526-06) in 990 µL of ice-cold extraction solvent (80% MeOH: 20% H<sub>2</sub>O containing 25 mM NEM and 10 mM ammonium formate, pH=7.0) containing 0.5 µM of [D<sub>4</sub>]-Homocysteine (Cambridge Isotope labs, Cat# DLM-8259-PK) followed by incubation at 4°C for 30 min. After centrifugation (17,000 g, 20 min, 4°C), the supernatants were analyzed by LC-MS following previously established conditions (Kang et al., 2019). For the chromatographic metabolite separation, a Vanquish UPLC system was coupled to a Q Exactive HF (QE-HF) mass spectrometer equipped with HESI (Thermo Fisher Scientific, Waltham, MA). The column was a SeQuant ZIC-pHILIC LC column, 5 mm, 150 x 4.6mm (MilliporeSigma, Burlington, MA) with a SeQuant ZIC-pHILIC guard column, 20 x 4.6 mm (MilliporeSigma, Burlington, MA). Mobile phase A was 10mM (NH<sub>4</sub>)<sub>2</sub>CO<sub>3</sub> and 0.05% NH<sub>4</sub>OH in H<sub>2</sub>O while mobile phase B was 100% ACN. The column chamber temperature was set to 30°C. The mobile phase condition was set according to the following gradient: 0-13min: 80% to 20% of mobile phase B, 13-15min: 20% of mobile phase B. The ESI ionization mode was positive. The MS scan range

(m/z) was set to 60-900. The mass resolution was 120,000 and the AGC target was  $3 \times 10^6$ . Capillary voltage and capillary temperature were set to 3.5 KV and 320°C, respectively. Five  $\mu\text{L}$  of sample was loaded. The homocysteine and [D<sub>4</sub>]-Homocysteine peaks were manually identified and integrated with EL-Maven (Version 0.11.0) by matching with an in-house library. Homocysteine levels were calculated using the standard curve and corrected using the [D<sub>4</sub>]-Homocysteine internal standard.

### **Metabolic Modeling**

Metabolic modeling simulations were performed with a Python script making use of the COBRApy toolkit (Ebrahim et al., 2013) and the ecYeastGEM\_batch model (Lu *et al.*, 2019), an “enzyme-constrained” variant (Sanchez et al., 2017) of Yeast8. The enzyme-constrained feature of the steady-state model is achieved by treating enzymes as metabolites that are temporarily “consumed” (i.e. removed from the available pool) while they are engaged in catalysis. The script first removes all preexisting reactions (which have not been experimentally validated) contributing to the “consumption” of YII058w (r\_0815No1, r\_0815REVNo1, and arm\_r\_0815). Second, the script adds the hypothetical homocysteine-generating reaction that we observe in our *in vitro* assay, which uses hydrogen sulfide and O-acetylhomoserine as substrates and yields homocysteine, acetate, and hydrogen as products, with YII058w as the catalyst. This reaction was added with a range of Kcat values assigned to YII058w in order to evaluate the “biomass” generated over a broad range of enzyme efficiencies. This reaction was made to be bidirectional. Thirdly, *MET15* was removed from the model, eliminating all reactions that the encoded enzyme was associated with. Finally, the model was

“solved” to obtain the flux through the biomass equation, a proxy for fitness. The reaction catalyzed by YII058w was made to be bidirectional; however, flux was only observed in the forward (homocysteine-producing) reaction. The default growth medium associated with the model, which contains sulfates but lacks organosulfurs, was used for all simulations.

### **Chelation of H<sub>2</sub>S with Ferric-EDTA sodium salt**

For each strain (FY4 and FY4-*met15Δ*), five single colonies were scraped from a YPDA agar plate and cells were resuspended in SD-Met+Glu medium. The optical density at 600 nm (OD<sub>600</sub>) of the suspension was measured using a spectrophotometer, and 25mL cultures were inoculated at a starting OD<sub>600</sub> of 0.1 in SD-Met+Glu or SD-Met+Glu supplemented with 0.048M Ferric(Fe)-EDTA (Ethylenediaminetetraacetic acid ferric sodium salt, E6067, Millipore Sigma) in 125mL Erlenmeyer flasks. The experiment was performed twice; each time, cultures were prepared in triplicate. Cultures were incubated at 30°C with 150rpm shaking and OD<sub>600</sub> was measured regularly for a period of ~51 hours. Cells were then pelleted to facilitate the exchange to fresh SD-Met+Glu medium, again using a starting OD<sub>600</sub> of 0.1, and incubated as before for 51 hours with regular OD<sub>600</sub> measurements. A portion of each culture was stored at 4°C. Ten µl drops of each culture (both the original culture and after the repassaged growth) were then both spotted and struck on agar plates (YPDA, SD-Met+Glu, SC-Met-Cys+Glu, SC-Met-Cys+Glu+Fe-EDTA and BiGGY) that were incubated at 30°C (Figure 4C) and imaged regularly with splmager Automated Imaging System (S & P Robotics Inc., Ontario, Canada).

## **Data availability**

All data generated/analyzed in this study is available in the main text, in the Supplementary Figures and Tables, and as Supplementary Data files. Supplementary material is available at <https://bit.ly/3pOe6aT>.

## **Code availability**

All images and statistical analysis within the main article and supplementary data were generated using code available at <https://github.com/sauriiin/methionine>.

## **ACKNOWLEDGEMENTS**

We thank all the members of the Carvunis Lab, and in particular Carly Houghton, for helpful suggestions during lab meetings and presentations. We also thank Kate Metedgul-Ernar, Cameron Hines and Brian Hsu for their precious help in the early stages of the project and S.G. Wendell and Steven Mullett for their assistance with mass spectrometry analysis.

## **FUNDING**

This work was supported by the National Institutes of Health grant R00GM108865 to A.-R.C, F32GM129929 to S.B.V.O, P01CA250984 to G.M.D, NIHS10OD023402 to S.G.W., and the AACR-Takeda Oncology Lung Cancer Research Fellowship (19-40-38-KANG) to Y.P.K.

## **AUTHOR CONTRIBUTIONS**

Conceptualization: S.B.V.O., S.B.P., N.C.C., G.M.D., A-R.C. Methodology: S.B.V.O., S.B.P., N.C.C., A.W., A.P.V., G.M.D., A-R.C. Investigation: S.B.V.O., S.B.P., N.C.C., A.W., I.B., M.M., J.X., Y.P.K., K.M.M., J.M., A.P.V. Writing: S.B.V.O., S.B.P., N.C.C., A.W., A-R.C. Review and Editing: S.B.V.O., S.B.P., N.C.C., T.I., A.P.V., G.M.D., A-R.C. Supervision: A-R.C.

## REFERENCES

Bean, G.J., Jaeger, P.A., Bahr, S., and Ideker, T. (2014). Development of ultra-high-density screening tools for microbial "omics". *PLoS One* 9, e85177.

10.1371/journal.pone.0085177.

Blackstone, E., Morrison, M., and Roth, M.B. (2005). H<sub>2</sub>S induces a suspended animation-like state in mice. *Science* 308, 518. 10.1126/science.1108581.

Boeke Lab (2003). The Met15 Resource: Update.

<http://www.bs.jhmi.edu/mbg/boekelab/Resources/Met15/Met15updt.html>.

Brachmann, C.B., Davies, A., Cost, G.J., Caputo, E., Li, J., Hieter, P., and Boeke, J.D. (1998). Designer deletion strains derived from *Saccharomyces cerevisiae* S288C: a useful set of strains and plasmids for PCR-mediated gene disruption and other applications. *Yeast* 14, 115-132. 10.1002/(SICI)1097-0061(19980130)14:2<115::AID-YEA204>3.0.CO;2-2.

Brewster, J.L., Pachl, P., McKellar, J.L.O., Selmer, M., Squire, C.J., and Patrick, W.M. (2021). Structures and kinetics of *Thermotoga maritima* MetY reveal new insights into the predominant sulfurylation enzyme of bacterial methionine biosynthesis. *J Biol Chem* 296, 100797. 10.1016/j.jbc.2021.100797.

Byrne, K.P., and Wolfe, K.H. (2005). The Yeast Gene Order Browser: combining curated homology and syntenic context reveals gene fate in polyploid species. *Genome Res* 15, 1456-1461. 10.1101/gr.3672305.

Chen, Z., Zhang, X., Li, H., Liu, H., Xia, Y., and Xun, L. (2018). The Complete Pathway for Thiosulfate Utilization in *Saccharomyces cerevisiae*. *Appl Environ Microbiol* 84. 10.1128/AEM.01241-18.

Cost, G.J., and Boeke, J.D. (1996). A useful colony colour phenotype associated with the yeast selectable/counter-selectable marker MET15. *Yeast* 12, 939-941.

10.1002/(SICI)1097-0061(199608)12:10%3C939::AID-YEA988%3E3.0.CO;2-L.

DiCarlo, J.E., Norville, J.E., Mali, P., Rios, X., Aach, J., and Church, G.M. (2013).

Genome engineering in *Saccharomyces cerevisiae* using CRISPR-Cas systems.

*Nucleic Acids Res* 41, 4336-4343. 10.1093/nar/gkt135.

Douglas, A.C., Smith, A.M., Sharifpoor, S., Yan, Z., Durbic, T., Heisler, L.E., Lee, A.Y.,

Ryan, O., Gottert, H., Surendra, A., et al. (2012). Functional analysis with a barcoder

yeast gene overexpression system. *G3 (Bethesda)* 2, 1279-1289.

10.1534/g3.112.003400.

Dunham, M.J., Gartenberg, M. R., Brown, G. W. (2015). *Methods in Yeast Genetics and*

*Genomics, 2015 Edition: A CSHL Course Manual (Cold Spring Harbor Laboratory Press).*

Ebrahim, A., Lerman, J.A., Palsson, B.O., and Hyduke, D.R. (2013). COBRApy:

COstraints-Based Reconstruction and Analysis for Python. *BMC Syst Biol* 7, 74.

10.1186/1752-0509-7-74.

Eddy, S.R. (2011). Accelerated Profile HMM Searches. *PLoS Comput Biol* 7, e1002195.

10.1371/journal.pcbi.1002195.

Endicott, M., Jones, M., and Hull, J. (2021). Amino acid metabolism as a therapeutic

target in cancer: a review. *Amino Acids* 53, 1169-1179. 10.1007/s00726-021-03052-1.

Ferguson, L.R., and von Borstel, R.C. (1992). Induction of the cytoplasmic 'petite'

mutation by chemical and physical agents in *Saccharomyces cerevisiae*. *Mutat Res*

265, 103-148. 10.1016/0027-5107(92)90042-z.

Gaensly, F., Picheth, G., Brand, D., and Bonfim, T.M. (2014). The uptake of different iron salts by the yeast *Saccharomyces cerevisiae*. *Braz J Microbiol* 45, 491-494.

10.1590/s1517-83822014000200016.

Giaever, G., and Nislow, C. (2014). The yeast deletion collection: a decade of functional genomics. *Genetics* 197, 451-465. 10.1534/genetics.114.161620.

Green, C.L., Lamming, D.W., and Fontana, L. (2021). Molecular mechanisms of dietary restriction promoting health and longevity. *Nat Rev Mol Cell Biol*. 10.1038/s41580-021-00411-4.

Hansen, J., and Johannesen, P.F. (2000). Cysteine is essential for transcriptional regulation of the sulfur assimilation genes in *Saccharomyces cerevisiae*. *Mol Gen Genet* 263, 535-542. 10.1007/s004380051199.

Hughes, C.E., Coody, T.K., Jeong, M.Y., Berg, J.A., Winge, D.R., and Hughes, A.L. (2020). Cysteine Toxicity Drives Age-Related Mitochondrial Decline by Altering Iron Homeostasis. *Cell* 180, 296-310 e218. 10.1016/j.cell.2019.12.035.

Johnson, J.E., and Johnson, F.B. (2014). Methionine restriction activates the retrograde response and confers both stress tolerance and lifespan extension to yeast, mouse and human cells. *PLoS One* 9, e97729. 10.1371/journal.pone.0097729.

Jumper, J., Evans, R., Pritzel, A., Green, T., Figurnov, M., Ronneberger, O., Tunyasuvunakool, K., Bates, R., Zidek, A., Potapenko, A., et al. (2021). Highly accurate protein structure prediction with AlphaFold. *Nature* 596, 583-589. 10.1038/s41586-021-03819-2.

Kang, Y.P., Torrente, L., Falzone, A., Elkins, C.M., Liu, M., Asara, J.M., Dibble, C.C., and DeNicola, G.M. (2019). Cysteine dioxygenase 1 is a metabolic liability for non-small cell lung cancer. *Elife* 8, e45572.

Lee, T.A., Jorgensen, P., Bognar, A.L., Peyraud, C., Thomas, D., and Tyers, M. (2010). Dissection of combinatorial control by the Met4 transcriptional complex. *Mol Biol Cell* 21, 456-469. 10.1091/mbc.E09-05-0420.

Lu, H., Li, F., Sanchez, B.J., Zhu, Z., Li, G., Domenzain, I., Marcisauskas, S., Anton, P.M., Lappa, D., Lieven, C., et al. (2019). A consensus *S. cerevisiae* metabolic model Yeast8 and its ecosystem for comprehensively probing cellular metabolism. *Nat Commun* 10, 3586. 10.1038/s41467-019-11581-3.

Madeira, F., Park, Y.M., Lee, J., Buso, N., Gur, T., Madhusoodanan, N., Basutkar, P., Tivey, A.R.N., Potter, S.C., Finn, R.D., and Lopez, R. (2019). The EMBL-EBI search and sequence analysis tools APIs in 2019. *Nucleic Acids Res* 47, W636-W641. 10.1093/nar/gkz268.

Masselot, M., and De Robichon-Szulmajster, H. (1975). Methionine biosynthesis in *Saccharomyces cerevisiae*. I. Genetical analysis of auxotrophic mutants. *Mol Gen Genet* 139, 121-132. 10.1007/BF00264692.

Nickerson, W.J. (1953). Reduction of inorganic substances by yeasts. I. Extracellular reduction of sulfite by species of *Candida*. *J Infect Dis* 93, 43-56. 10.1093/infdis/93.1.43.

Ono, B., Ishii, N., Fujino, S., and Aoyama, I. (1991). Role of hydrosulfide ions (HS<sup>-</sup>) in methylmercury resistance in *Saccharomyces cerevisiae*. *Appl Environ Microbiol* 57, 3183-3186. 10.1128/aem.57.11.3183-3186.1991.

- Ono, B., Shirahige, Y., Nanjoh, A., Andou, N., Ohue, H., and Ishino-Arao, Y. (1988). Cysteine biosynthesis in *Saccharomyces cerevisiae*: mutation that confers cystathionine beta-synthase deficiency. *J Bacteriol* *170*, 5883-5889. 10.1128/jb.170.12.5883-5889.1988.
- Parikh, S.B., Castilho Coelho, N., and Carvunis, A.R. (2021). LI Detector: a framework for sensitive colony-based screens regardless of the distribution of fitness effects. *G3 (Bethesda)* *11*. 10.1093/g3journal/jkaa068.
- Petti, A.A., Crutchfield, C.A., Rabinowitz, J.D., and Botstein, D. (2011). Survival of starving yeast is correlated with oxidative stress response and nonrespiratory mitochondrial function. *Proc Natl Acad Sci U S A* *108*, E1089-1098. 10.1073/pnas.1101494108.
- Philip, C.V., and Brooks, D.W. (1974). Iron(III) chelate complexes of hydrogen sulfide and mercaptans in aqueous solution. *Inorganic Chemistry* *13*, 384-386. 10.1021/ic50132a030.
- Plummer, J.D., and Johnson, J.E. (2019). Extension of Cellular Lifespan by Methionine Restriction Involves Alterations in Central Carbon Metabolism and Is Mitophagy-Dependent. *Front Cell Dev Biol* *7*, 301. 10.3389/fcell.2019.00301.
- Raymond, R.K., Kastanos, E.K., and Appling, D.R. (1999). *Saccharomyces cerevisiae* expresses two genes encoding isozymes of methylenetetrahydrofolate reductase. *Arch Biochem Biophys* *372*, 300-308. 10.1006/abbi.1999.1498.
- Ryan, O.W., Skerker, J.M., Maurer, M.J., Li, X., Tsai, J.C., Poddar, S., Lee, M.E., DeLoache, W., Dueber, J.E., Arkin, A.P., and Cate, J.H. (2014). Selection of

chromosomal DNA libraries using a multiplex CRISPR system. *Elife* 3.

10.7554/eLife.03703.

Sanchez, B.J., Zhang, C., Nilsson, A., Lahtvee, P.J., Kerkhoven, E.J., and Nielsen, J. (2017). Improving the phenotype predictions of a yeast genome-scale metabolic model by incorporating enzymatic constraints. *Mol Syst Biol* 13, 935. 10.15252/msb.20167411.

Shen, X.X., Ofulente, D.A., Kominek, J., Zhou, X., Steenwyk, J.L., Buh, K.V., Haase, M.A.B., Wisecaver, J.H., Wang, M., Doering, D.T., et al. (2018). Tempo and Mode of Genome Evolution in the Budding Yeast Subphylum. *Cell* 175, 1533-1545 e1520.

10.1016/j.cell.2018.10.023.

Singh, A., and Sherman, F. (1974). Association of methionine requirement with methyl mercury resistant mutants of yeast. *Nature* 247, 227-229. 10.1038/247227a0.

Sprouffske, K., and Wagner, A. (2016). Growthcurver: an R package for obtaining interpretable metrics from microbial growth curves. *BMC Bioinformatics* 17, 172.

10.1186/s12859-016-1016-7.

Stanford University (2020). *Saccharomyces Genome Database*.

<https://www.yeastgenome.org/>.

Team, R.C. (2021). R: A language and environment for statistical computing. (R Foundation for Statistical Computing, Vienna, Austria.).

Thomas, D., and Surdin-Kerjan, Y. (1997). Metabolism of sulfur amino acids in *Saccharomyces cerevisiae*. *Microbiol Mol Biol Rev* 61, 503-532.

Van Oss, S.B., Shirra, M.K., Bataille, A.R., Wier, A.D., Yen, K., Vinayachandran, V., Byeon, I.L., Cucinotta, C.E., Heroux, A., Jeon, J., et al. (2016). The Histone Modification

Domain of Paf1 Complex Subunit Rtf1 Directly Stimulates H2B Ubiquitylation through an Interaction with Rad6. *Mol Cell* 64, 815-825. 10.1016/j.molcel.2016.10.008.

Vowinckel, J., Hartl, J., Marx, H., Kerick, M., Runggatscher, K., Keller, M.A., Mulleder, M., Day, J., Weber, M., Rinnerthaler, M., et al. (2021). The metabolic growth limitations of petite cells lacking the mitochondrial genome. *Nat Metab* 3, 1521-1535.

10.1038/s42255-021-00477-6.

Walvekar, A.S., and Laxman, S. (2019). Methionine at the Heart of Anabolism and Signaling: Perspectives From Budding Yeast. *Front Microbiol* 10, 2624.

10.3389/fmicb.2019.02624.

Wilson, D., Pethica, R., Zhou, Y., Talbot, C., Vogel, C., Madera, M., Chothia, C., and Gough, J. (2009). SUPERFAMILY--sophisticated comparative genomics, data mining, visualization and phylogeny. *Nucleic Acids Res* 37, D380-386. 10.1093/nar/gkn762.

Winston, F., Dollard, C., and Ricupero-Hovasse, S.L. (1995). Construction of a set of convenient *Saccharomyces cerevisiae* strains that are isogenic to S288C. *Yeast* 11, 53-55. 10.1002/yea.320110107.

Yamagata, S. (1971). Homocysteine synthesis in yeast. Partial purification and properties of O-acetylhomoserine sulfhydrylase. *J Biochem* 70, 1035-1045.

10.1093/oxfordjournals.jbchem.a129712.

Yamagata, S. (1976). O-Acetylserine and O-acetylhomoserine sulfhydrylase of yeast. Subunit structure. *J Biochem* 80, 787-797. 10.1093/oxfordjournals.jbchem.a131339.

Zhang, N., Merlotti, C., Wu, J., Ismail, T., El-Moghazy, A.N., Khan, S.A., Butt, A.,

Gardner, D.C., Sims, P.F., and Oliver, S.G. (2001). Functional Analysis of six novel

ORFs on the left arm of Chromosome XII of *Saccharomyces cerevisiae* reveals three of

them responding to S-starvation. *Yeast* *18*, 325-334. 10.1002/1097-

0061(20010315)18:4<325::AID-YEA669>3.0.CO;2-K.

Zou, K., Ouyang, Q., Li, H., and Zheng, J. (2017). A global characterization of the translational and transcriptional programs induced by methionine restriction through ribosome profiling and RNA-seq. *BMC Genomics* *18*, 189. 10.1186/s12864-017-3483-2.

## SUPPLEMENTARY MATERIAL

### SUPPLEMENTARY FIGURES

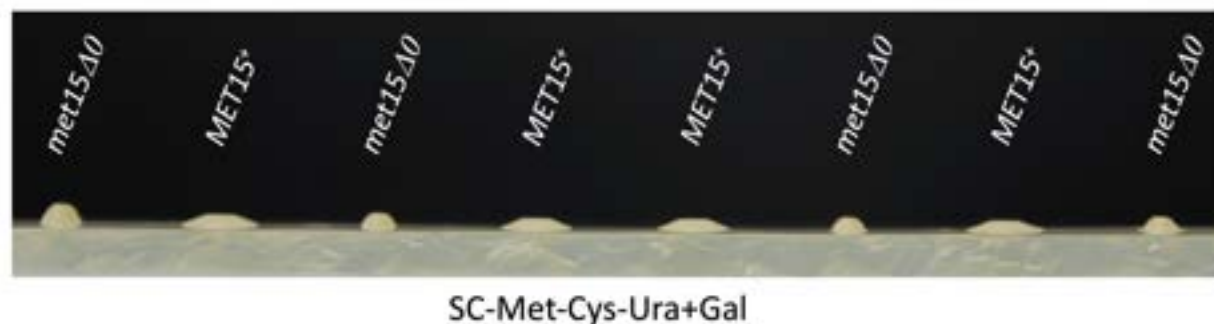


**Figure S1. Loss of *MET15* strongly influences colony morphology.** Sectional dissection of an agar plate showing colonies from a BY4741 (*met15Δ*) strain that carries a *URA3*-marked vector plasmid and the same strain carrying a *MET15* overexpression plasmid (*MET15<sup>+</sup>*) growing on SC-Met-Cys-Ura+Gal solid agar medium for ~5 days. Colonies formed from cells lacking *MET15* have a markedly different morphology than those formed from *MET15<sup>+</sup>* cells.

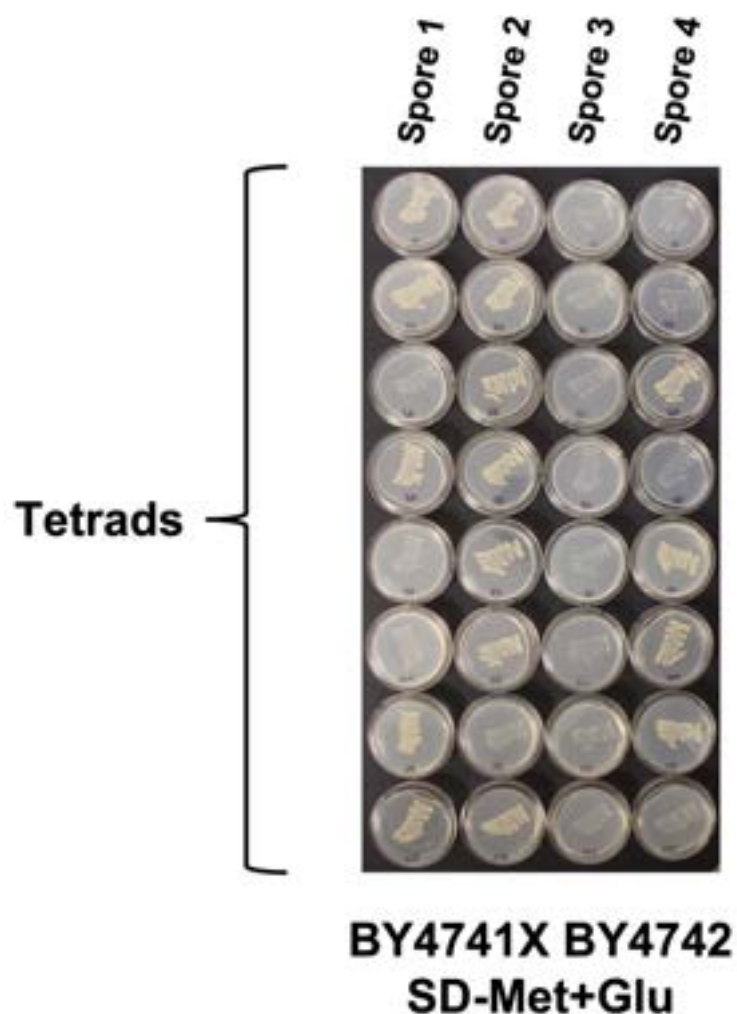


**Figure S2. *met15* $\Delta$ -associated growth phenotype segregates 2:2 in a heterozygous cross.** The BY4741 and BY4742 strains were mated, sporulated, and dissected using standard techniques. Eight four-spore tetrads were grown on YPDA, and then patched onto SD-Met+Glu medium. Individual plates were used to prevent cross-feeding between *MET15*<sup>+</sup> and *met15* $\Delta$  cells. Each tetrad resulted in 2:2 segregation of the growth phenotype on organosulfur-deficient media. Notably, the growth of *met15* $\Delta$  thick patches was substantially weaker than that observed in the high-density pinning assays used throughout most of the manuscript.

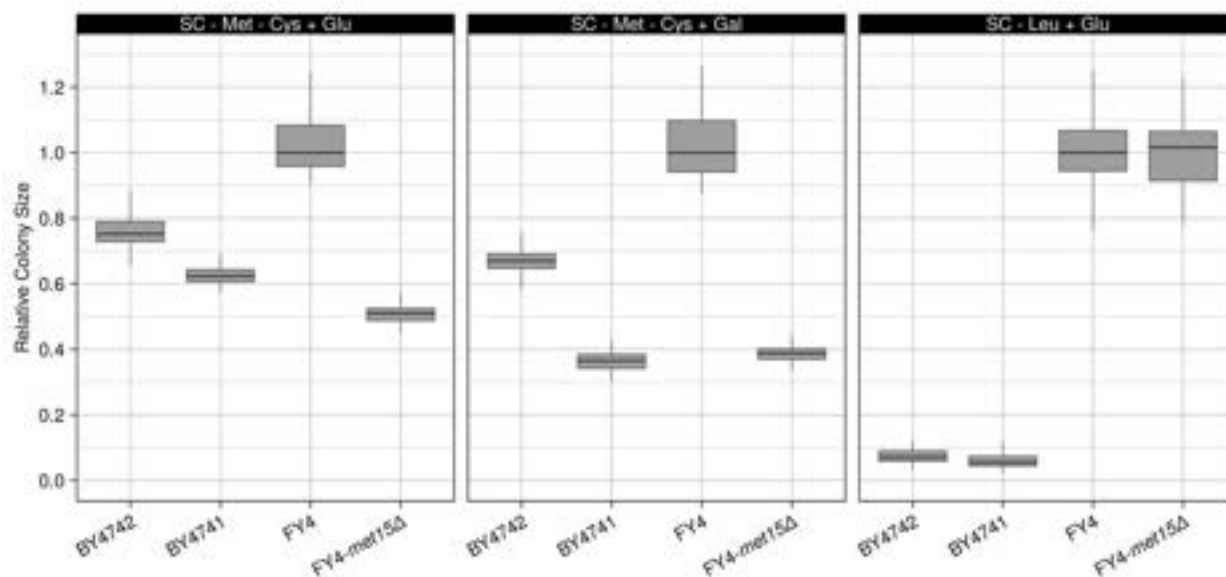


**Figure S3. *met15Δ* cells also grow robustly in “synthetic complete” (SC) media lacking organosulfurs.** The same pinning and analysis pipeline shown in **Figure 1A-C** was repeated but on SC-Met-Cys media containing either glucose or galactose as the sole carbon source, or on SC-Leu+Glu medium, where the negligible growth of the BY4741 and BY4742 strains is consistent with auxotrophy. The prototrophic strain FY4 and a mutant derivative lacking *MET15* were also assayed. Cells were grown for 140 hours (SC-Leu+Glu) or 165 hours (SC-Met+Glu/Gal).

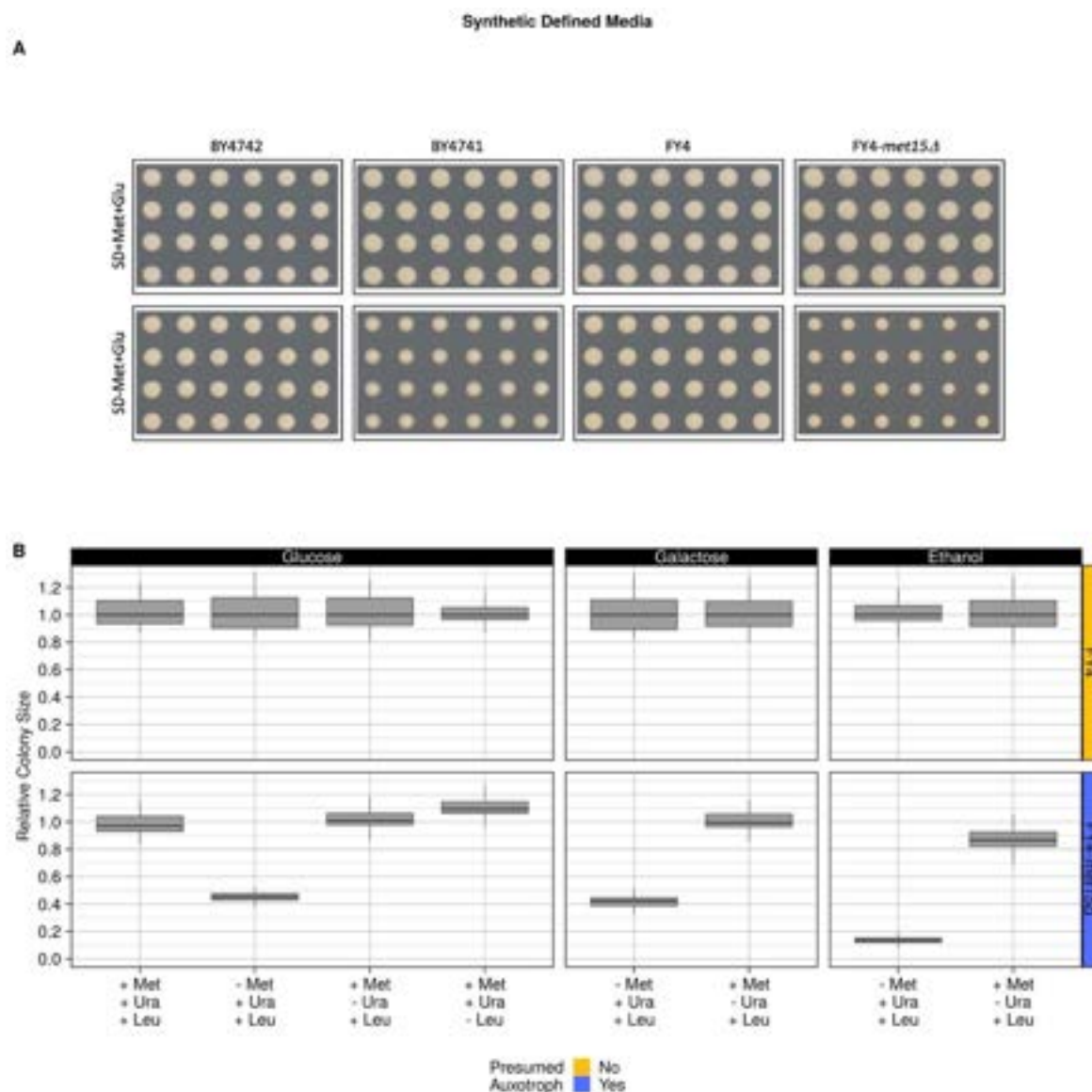


**Figure S4. Robust growth of *met15Δ* cells in an organosulfur-deficient medium.**

**A)** In “synthetic defined” medium lacking methionine and with glucose comprising the carbon source (SD-Met+Glu), cells harboring the *met15Δ0* deletion (BY4741) or a “scarless deletion” of *MET15* made by CRISPR (FY4-*met15Δ*) show surprisingly robust growth inconsistent with their presumed auxotrophy, while in “conventional” SD medium (SD+Met+Glu), these mutant cells form slightly larger colonies than their nearly isogenic *MET15*<sup>+</sup> counterparts. Colonies shown here have grown for 366 hours. **B)** The “scarless” CRISPR *met15Δ* mutant shows similarly robust growth, inconsistent with auxotrophy, when glucose or galactose comprise the carbon source, but growth is much weaker when the same strain is grown with ethanol as the carbon source. Data associated with each plot is drawn from two 384-colony density plates for each strain made as described in **Figure 1A**. Pixel counts for each colony were normalized to obtain the median colony relative to FY4 grown in the same condition (**Experimental Procedures**). Cells were grown for ~358 to 366 hours.

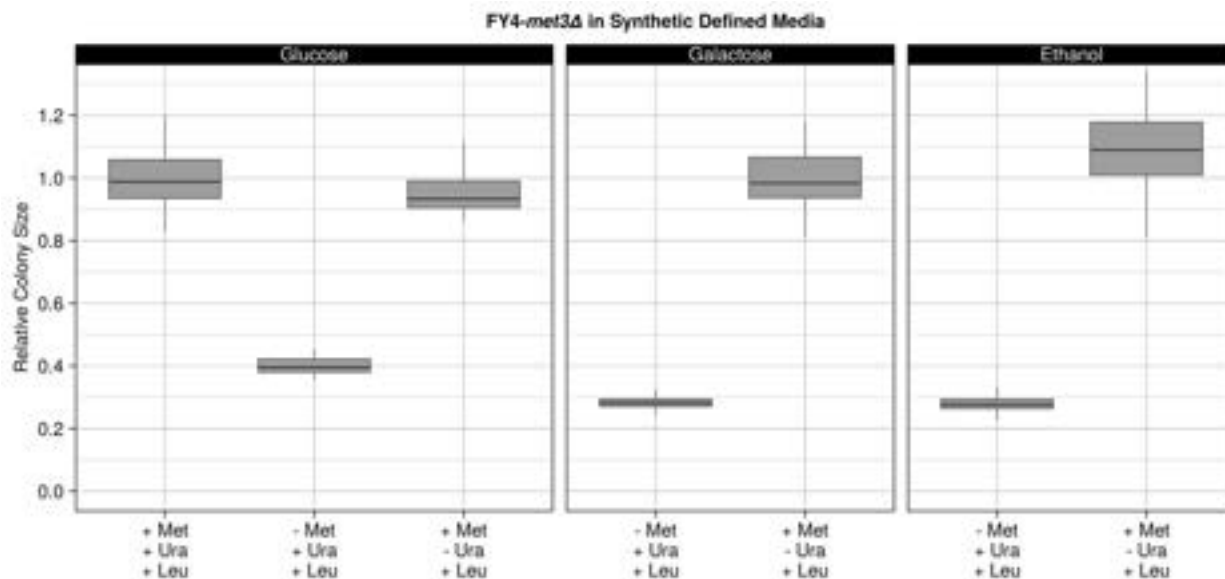


**Figure S5. The growth of FY4-*met3Δ* cells on SD-Met media is generally unaffected by the carbon source.** The FY4-*met3Δ* mutant was grown in the same manner as the strains presented in **Figures 1C** and **S4A-B**. Colony size (pixel count) data associated with each plot is drawn from two 384-colony density plates for each strain made as described in **Figure 1A**. Pixel counts for each colony were normalized to obtain the median colony relative to FY4 grown in the same condition (**Experimental Procedures**). Colonies shown here have grown for 366 hours.

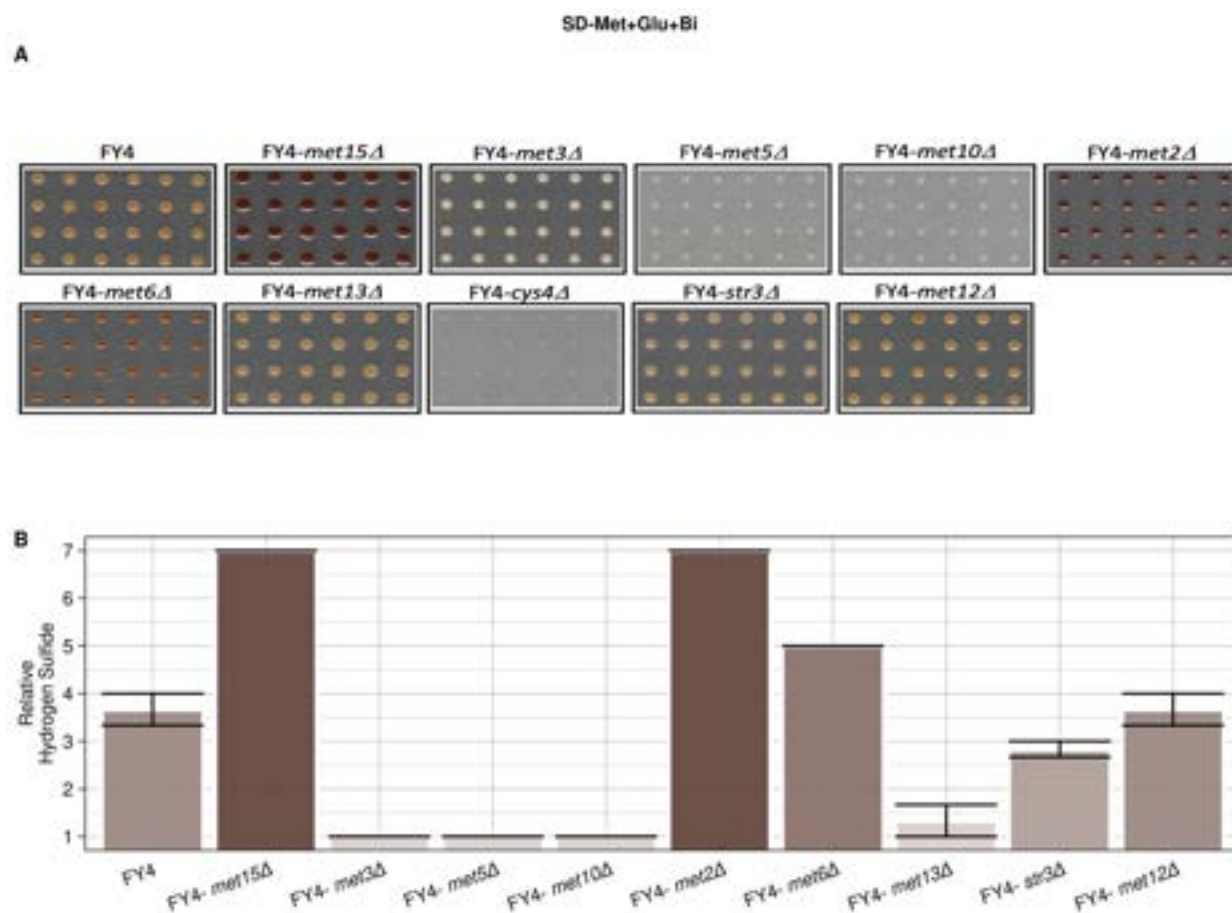


**Figure S6. H<sub>2</sub>S levels of mutant strains in an organosulfur-free medium.** Cropped images (Panel A) and qualitative assessment of colony color (Panel B, performed in the same manner described in **Figure 2D**) of the mutant strains tested in **Figures 2B-D** and **S5** pinned to SD-Met+Glu medium containing bismuth (SD-Met+Glu+Bi). The FY4-*cys4Δ* mutant showed no observable growth hence has been excluded from Panel B. The darkness of the colonies is a proxy for the level of excess H<sub>2</sub>S in each strain.

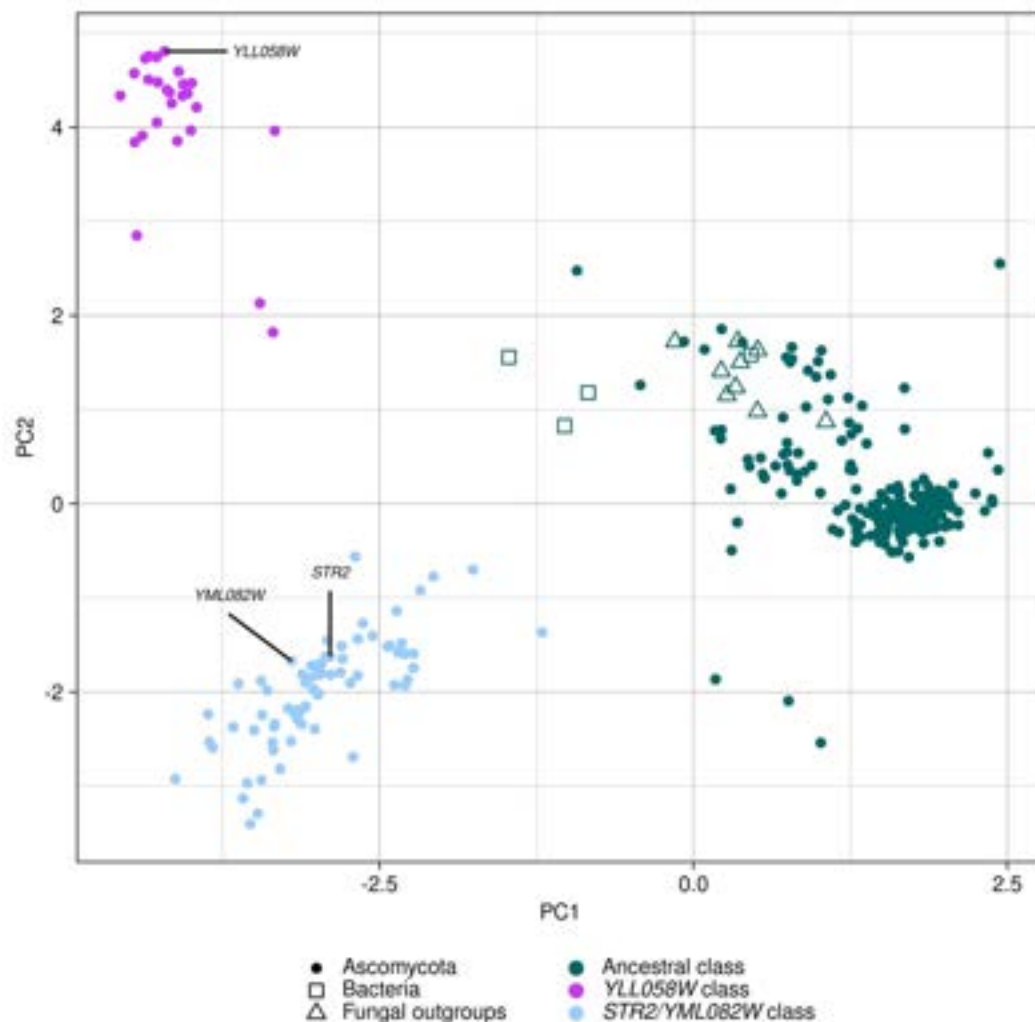


**Figure S7. YLL058W homologs cluster into three distinct classes.** The sequence distances between YLL058W homologs found in budding yeasts and outgroup taxa are visualized using multidimensional scaling (MDS). Points are colored according to k-means clustering based on these sequence distances using three clusters. The three genes contained in the *S. cerevisiae* genome are labeled.

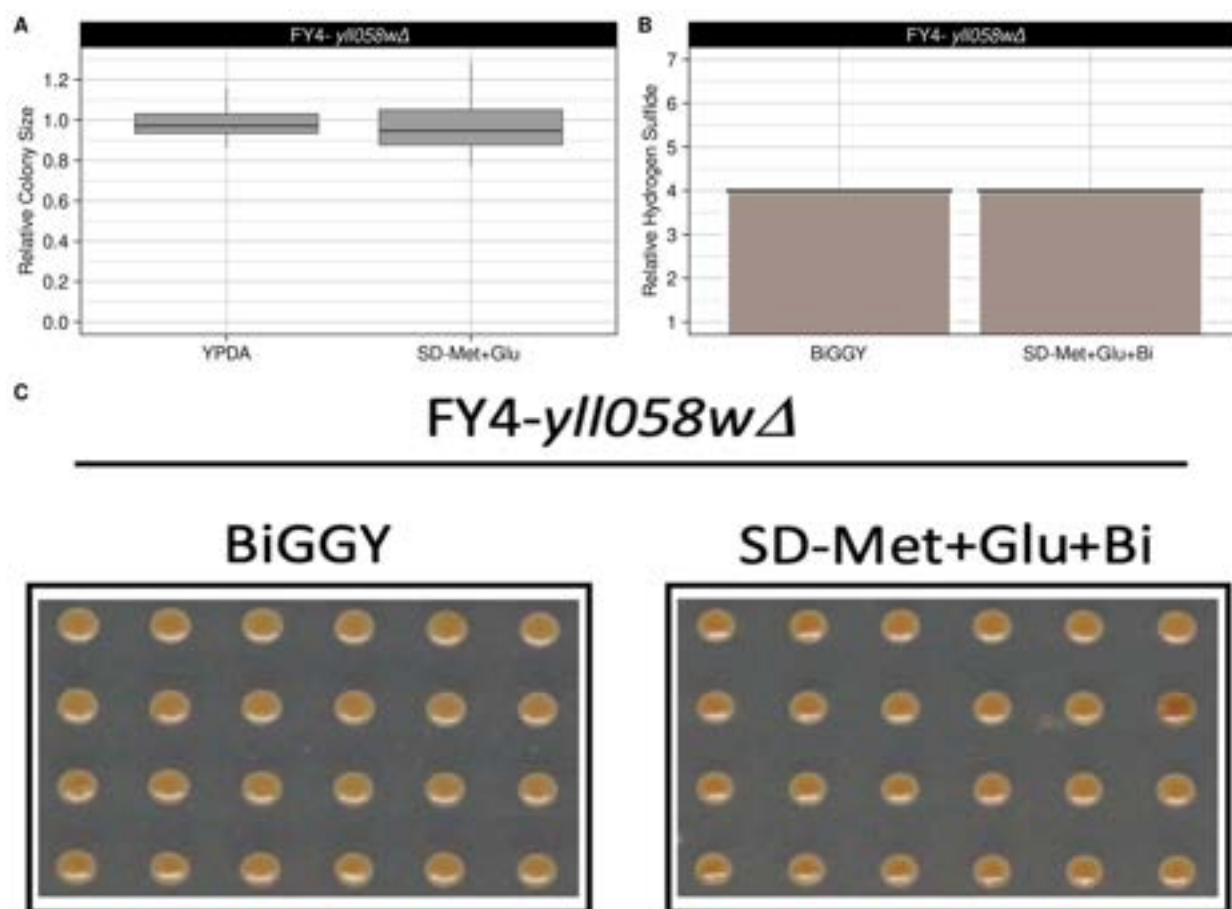


**Figure S8. Deletion of *YLL058W* has negligible effect on fitness and H<sub>2</sub>S accumulation in the FY4 background.** **A)** Deletion of *YLL058W* in the prototrophic FY4 background has a negligible effect on growth in SD-Met+Glu medium. The strains were examined in the same manner as the mutants shown in **Figure 2B**, with colony size normalized to that of FY4. **B and C)** The relative H<sub>2</sub>S level of FY4-*yll058wΔ*, as determined by growth on BiGGY and SD-Met+Glu+Bi, is comparable to that of wild-type FY4 cells. For Panel B, the darkness of the colonies was scored on the same qualitative scale applied to the mutants in **Figures 2C-D and S6B**.

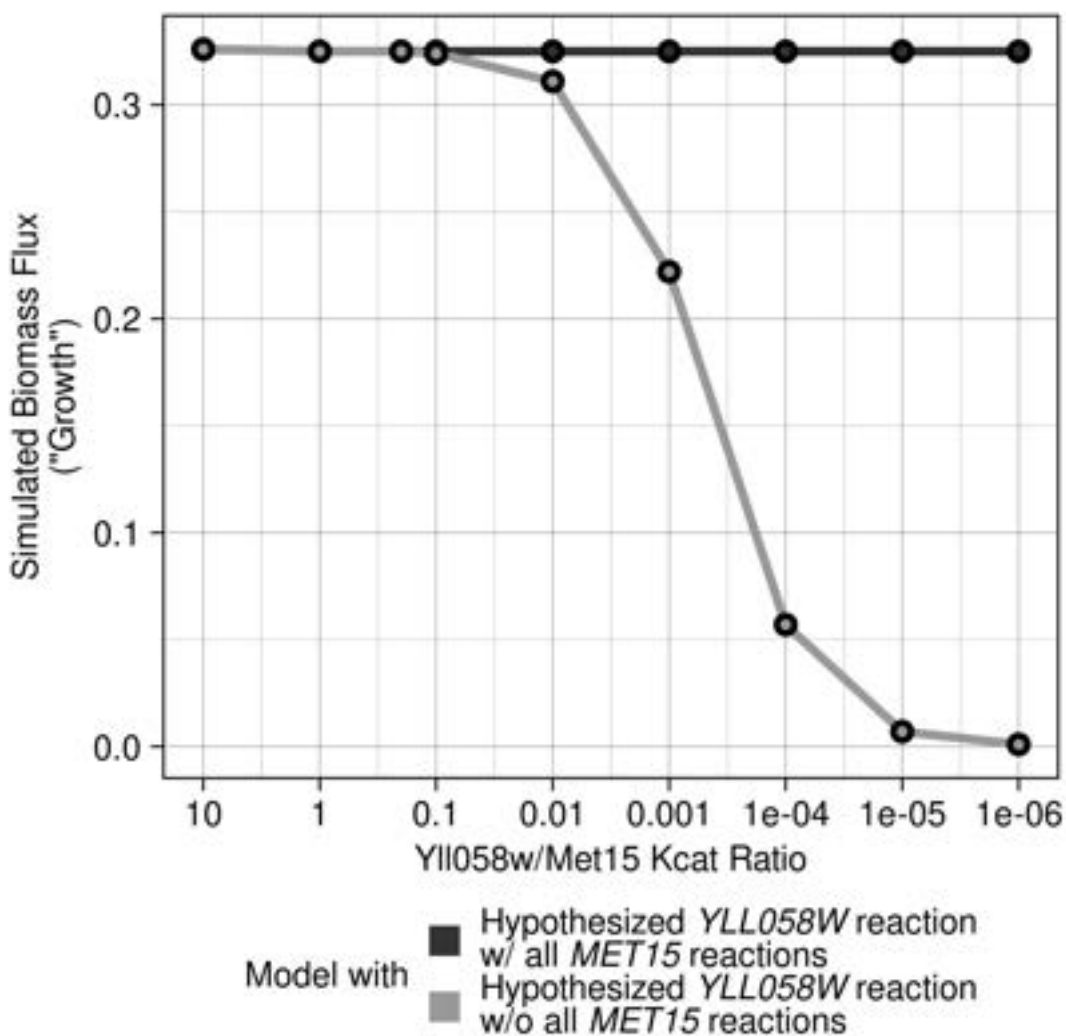


**Figure S9. Simulated growth utilizing the consensus, genome-scale *S. cerevisiae* metabolic model (Lu et al., 2019) shows that a low-efficiency homocysteine synthase can support growth.** Two modifications were made to the default model – the addition of the *in vitro* reaction carried out in **Figure 3E** utilizing YII058w as the catalytic enzyme (black), and the subsequent removal of the *MET15* gene from the model (gray). The x-axis indicates the flux through the “biomass equation”, a proxy for growth/fitness, and the y-axis indicates different catalytic efficiency (Kcat) values assigned to YII058w in the added reaction, with the efficiency of YII058w in the hypothetical reaction decreasing from left to right.

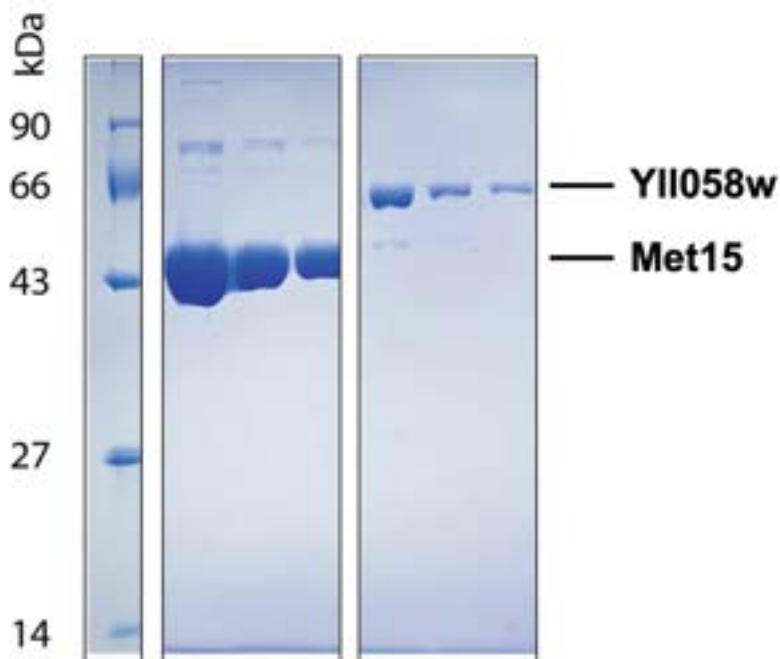


**Figure S10. Coomassie-stained SDS-PAGE gel showing the final fractions that contained the recombinantly-expressed, purified protein used in the *in vitro* homocysteine biosynthesis assay.** A lane containing molecular weight standards (kDa = kilodaltons) is shown on the left. Lanes containing less pure fractions that were not used were cropped, but the image is otherwise unaltered.

## SUPPLEMENTARY TABLES

**Table S1.** Settings for the RoToR HDA robotic plate handler used for all of the automated pinning experiments described in the manuscript. Screening of the deletion collection involved all five unique settings, while the remaining pinning experiments all followed the general schema described in **Figure 1B** and used only the “384 Glycerol to 384 Plate” and “384 Plate to 384 Plate” settings.

| SETTINGS         |                  |              | 384 Glycerol to 384 Plate | 384 Plate to 384 Plate | 384 Plate to 1536 Plate | 1536 Plate to 1536 Plate | 1536 Plate to 6144 Plate |
|------------------|------------------|--------------|---------------------------|------------------------|-------------------------|--------------------------|--------------------------|
| Source           |                  |              | 384 MTP                   | 384 Agar               | 384 Agar                | 1536 Agar                | 1536 Agar                |
| Target           |                  |              | 384 Agar                  | 384 Agar               | 1536 Agar               | 1536 Agar                | 6144 Agar                |
| Pads             |                  |              | 384 Long Pin              | 384 Short              | 384 Short               | 1536 Short               | 1536 Short               |
| Program          |                  |              | Spot Many                 | Replicate              | 1-4 Array               | Replicate                | 1-4 Array                |
| General          |                  |              |                           |                        |                         |                          |                          |
|                  | Quantity         |              | 2                         | N/A                    | N/A                     | N/A                      | N/A                      |
|                  | Recycle          |              | None                      | None                   | None                    | None                     | None                     |
|                  | Plate Protection |              | Uncheck                   | Uncheck                | Uncheck                 | Uncheck                  | Uncheck                  |
|                  | Pairs            |              |                           |                        |                         |                          |                          |
|                  | Start Pair       |              |                           |                        |                         |                          |                          |
| Source           |                  |              |                           |                        |                         |                          |                          |
|                  | Offset           |              |                           | Automatic<br>0.4 mm    | Automatic<br>0.4 mm     | Automatic<br>0.3 mm      | Automatic<br>0.3 mm      |
|                  | Offsets...       | Max Radius   |                           |                        |                         |                          |                          |
|                  | Pinning          |              |                           |                        |                         |                          |                          |
|                  |                  | Pin Pressure |                           | 32%                    | 32%                     | 58%                      | 58%                      |
|                  |                  | Speed        | 19 mm per sec             | 19 mm per sec          | 19 mm per sec           | 19 mm per sec            | 19 mm per sec            |
|                  |                  | Backoff      | 0.5 mm                    | 2 mm                   | 2 mm                    | 2.5 mm                   | 2 mm                     |
|                  |                  | Repeat Pin   | 1 times                   | 1 times                | 1 times                 | 1 times                  | 1 times                  |
|                  | Dry Mix          |              |                           |                        |                         |                          |                          |
|                  |                  | Clearance    |                           | 0.5 mm                 | 0.5 mm                  | 0.5 mm                   | 0.5 mm                   |
|                  |                  | Diameter     |                           | 1 mm                   | 1 mm                    | 1 mm                     | 1 mm                     |
|                  |                  | Cycles       |                           | 1 rotations            | 1 rotations             | 1 rotations              | 1 rotations              |
|                  | Wet Mix          |              |                           |                        |                         |                          |                          |
|                  |                  | Diameter     | 1 mm                      |                        |                         |                          |                          |
|                  |                  | Speed        | 25 mm per sec             |                        |                         |                          |                          |
|                  |                  | Cycles       | 3 rotations               |                        |                         |                          |                          |
|                  |                  | Travel       | 3                         |                        |                         |                          |                          |
|                  |                  |              | 2D/3D                     |                        |                         |                          |                          |
|                  | Permanent Offset |              | 3D                        |                        |                         |                          |                          |
| Target           |                  |              |                           |                        |                         |                          |                          |
|                  | Pinning          |              |                           |                        |                         |                          |                          |
|                  |                  | Pin Pressure | 32%                       | 32%                    | 32%                     | 58%                      | 58%                      |
|                  |                  | Speed        | 19 mm per sec             | 19 mm per sec          | 19 mm per sec           | 19 mm per sec            | 19 mm per sec            |
|                  |                  | Backoff      |                           |                        |                         |                          |                          |
|                  |                  | Overshoot    | 2 mm                      | 2 mm                   | 2 mm                    | 2 mm                     | 2 mm                     |
|                  |                  | Repeat Pin   | 1 times                   | 1 times                | 1 times                 | 1 times                  | 1 times                  |
|                  | Dry Mix          |              |                           |                        |                         |                          |                          |
|                  |                  | Clearance    | 0.5 mm                    | 0.5 mm                 | 0.5 mm                  | 0.4 mm                   | 0.5 mm                   |
|                  |                  | Diameter     | 1 mm                      | 1 mm                   | 1 mm                    | 1 mm                     | 1 mm                     |
|                  |                  | Cycles       | 1 rotations               | 1 rotations            | 1 rotations             | 1 rotations              | 1 rotations              |
|                  | Wet Mix          |              |                           |                        |                         |                          |                          |
|                  |                  | Diameter     |                           |                        |                         |                          |                          |
|                  |                  | Speed        |                           |                        |                         |                          |                          |
|                  |                  | Cycles       |                           |                        |                         |                          |                          |
|                  |                  | Travel       |                           |                        |                         |                          |                          |
|                  |                  |              | 2D/3D                     |                        |                         |                          |                          |
| Pads             |                  |              |                           |                        |                         |                          |                          |
|                  | Pressure         |              |                           |                        |                         |                          |                          |
|                  | Eject Time       |              |                           |                        |                         |                          |                          |
| Selected Options |                  |              |                           |                        |                         |                          |                          |
|                  | Recycle          |              | Off                       | Off                    |                         | Off                      |                          |
|                  | Revisit          |              | Off                       | Off                    |                         | Off                      |                          |
|                  | Protect Source   |              | Off                       | Off                    | Off                     | Off                      | Off                      |
|                  | Offset           |              |                           | Auto                   | Auto                    | Auto                     | Auto                     |
|                  | Source Mix       |              | On                        | On                     | Off                     | Off                      | Off                      |
|                  | Target Mix       |              | On                        | Off                    | Off                     | Off                      | Off                      |

**Table S2.** Mass spectrometry analysis confirms that the growth medium is not contaminated with organosulfurs. ND= Not Detected.

|                       | Cysteine | Methionine | Homocysteine | SAM |
|-----------------------|----------|------------|--------------|-----|
| Yeast Nitrogen Base   | ND       | ND         | ND           | ND  |
| 2% Glucose            | ND       | ND         | ND           | ND  |
| Leucine               | ND       | ND         | ND           | ND  |
| Histidine             | ND       | ND         | ND           | ND  |
| Uracil                | ND       | ND         | ND           | ND  |
| Lysine                | ND       | ND         | ND           | ND  |
| Glutamic Acid         | ND       | ND         | ND           | ND  |
| SD-Met                | ND       | ND         | ND           | ND  |
| SD+Met                | ND       | 7.15 mM    | ND           | ND  |
| ddH <sub>2</sub> O    | ND       | ND         | ND           | ND  |
| Pure H <sub>2</sub> O | ND       | ND         | ND           | ND  |

**Table S3.** *YLL058W* and its orthologs are found in a cluster of genes near the telomere. *S. cerevisiae* gene names are used for all species shown. The ten nearest genes (5' upstream (5') genes, numbered -1 to -5, and 5 downstream (3') genes, numbered 1 to 5) to *YLL058W* orthologs are shown. Asterisks indicate a known role in sulfur metabolism.

| Species                           | Position Relative to <i>YLL058W</i> |               |               |                |               |                  |                  |                |               |                |                |
|-----------------------------------|-------------------------------------|---------------|---------------|----------------|---------------|------------------|------------------|----------------|---------------|----------------|----------------|
|                                   | -5                                  | -4            | -3            | -2             | -1            | <i>YLL058W</i>   | 1                | 2              | 3             | 4              | 5              |
| <i>Saccharomyces cerevisiae</i>   | <i>PAU18</i>                        | <i>AYT1</i>   | <i>MHT1</i> * | <i>MMP1</i> *  | <i>GTT2</i> * | <i>YLL058W</i> * | <i>JLP1</i> *    | <i>YLL056C</i> | <i>YCT1</i> * | <i>YLL054C</i> | <i>YLL053C</i> |
| <i>Zygosaccharomyces bisporus</i> | <i>RRP42</i>                        | <i>TRM3</i>   | <i>ATG20</i>  | <i>YDL114W</i> | <i>ARG8</i>   | <i>YLL058W</i> * | <i>YLL058W</i> * | <i>YCT1</i> *  | <i>AYR1</i>   | <i>DAL5</i>    | <i>PUT3</i>    |
| <i>Torulopsis delbrueckii</i>     | <i>RPT6</i>                         | <i>ALG23</i>  | <i>DSE4</i>   | <i>MHT1</i> *  | <i>MMP1</i> * | <i>YLL058W</i> * | <i>YCT1</i> *    | <i>DLD2</i>    | <i>GRX1</i> * | <i>DIPS</i>    | <i>YRF1-J</i>  |
| <i>Torulopsis pretoriensis</i>    | <i>THI73</i>                        | <i>AMD2</i>   | <i>SOA1</i> * | <i>JLP1</i> *  | <i>PHO84</i>  | <i>YLL058W</i> * | <i>MMP1</i> *    | <i>MHT1</i> *  | <i>DSE4</i>   | <i>ALG23</i>   | <i>RPT6</i>    |
| <i>Lachancea quebecensis</i>      | <i>YCT1</i> *                       | <i>SOA1</i> * | <i>ZRT1</i>   | <i>PHO11</i>   | <i>ZPS1</i>   | <i>YLL058W</i> * | <i>VEL1</i>      | <i>FLO5</i>    | <i>COS9</i>   | <i>AIF1</i>    | <i>YER152C</i> |

**Table S4.** OD<sub>600</sub> values at saturation (~51 hours) for cultures of the indicated strains grown in SD-Met+Glu medium with or without the H<sub>2</sub>S chelator Ferric(Fe)-EDTA (column 4), and OD<sub>600</sub> values for the same cultures diluted and re-passaged in SD-Met-Glu medium lacking chelator (column 5). Each strain has 3 replicates (1-3) from two independent experiments (A&B). Although FY4-*met15Δ* cultures generally failed to show any substantial growth in liquid medium without an H<sub>2</sub>S chelator present (**Figure 4B**), we occasionally observed “escape” in four FY4-*met15Δ* cultures (indicated in green text) grown in SD-Met+Glu without an H<sub>2</sub>S chelator present, independent of whether the cells had previously been in the presence of chelator.

| Strain             | Replicate | Initial Medium     | OD600 | OD600 (Repassage) |
|--------------------|-----------|--------------------|-------|-------------------|
| FY4                | 1A        | SD-Met+Glu         | 4.98  | 6.13              |
| FY4                | 1B        | SD-Met+Glu         | 5.45  | 4.75              |
| FY4                | 2A        | SD-Met+Glu         | 4.9   | 5.88              |
| FY4                | 2B        | SD-Met+Glu         | 5.71  | 4.64              |
| FY4                | 3A        | SD-Met+Glu         | 5.13  | 6.45              |
| FY4                | 3B        | SD-Met+Glu         | 5.76  | 5.8               |
| FY4                | 1A        | SD-Met+Glu+Fe-EDTA | 5.86  | 7.71              |
| FY4                | 1B        | SD-Met+Glu+Fe-EDTA | 6.76  | 7.03              |
| FY4                | 2A        | SD-Met+Glu+Fe-EDTA | 5.5   | 7.82              |
| FY4                | 2B        | SD-Met+Glu+Fe-EDTA | 6.24  | 6.78              |
| FY4                | 3A        | SD-Met+Glu+Fe-EDTA | 5.26  | 7.87              |
| FY4                | 3B        | SD-Met+Glu+Fe-EDTA | 6.15  | 6.61              |
| FY4- <i>met15Δ</i> | 1A        | SD-Met+Glu         | 1.39  | 0.48              |
| FY4- <i>met15Δ</i> | 1B        | SD-Met+Glu         | 0.21  | 0.09              |
| FY4- <i>met15Δ</i> | 2A        | SD-Met+Glu         | 0.29  | 5.93              |
| FY4- <i>met15Δ</i> | 2B        | SD-Met+Glu         | 0.22  | 0.07              |
| FY4- <i>met15Δ</i> | 3A        | SD-Met+Glu         | 0.34  | 0.14              |
| FY4- <i>met15Δ</i> | 3B        | SD-Met+Glu         | 0.21  | 0.07              |
| FY4- <i>met15Δ</i> | 1A        | SD-Met+Glu+Fe-EDTA | 2.55  | 0.39              |
| FY4- <i>met15Δ</i> | 1B        | SD-Met+Glu+Fe-EDTA | 1.02  | 3.29              |
| FY4- <i>met15Δ</i> | 2A        | SD-Met+Glu+Fe-EDTA | 2.23  | 0.26              |
| FY4- <i>met15Δ</i> | 2B        | SD-Met+Glu+Fe-EDTA | 0.56  | 0.08              |
| FY4- <i>met15Δ</i> | 3A        | SD-Met+Glu+Fe-EDTA | 2.52  | 4.22              |
| FY4- <i>met15Δ</i> | 3B        | SD-Met+Glu+Fe-EDTA | 1.12  | 3.32              |

**Table S5.** Kruskal-Wallis Test results comparing the growth of a given strain in condition\_1 (+Met) vs. condition\_2 (-Met), with EtOH or Glucose. The statistic and p-value columns are the Kruskal-Wallis test statistic and p-value output, and the effect size column is the difference between the median fitness value in media lacking methionine and that in media containing methionine divided by the median fitness value in media containing methionine.

| Strain                                 | condition_1 (+Met) | condition_2 (-Met) | statistic | p-value | effect size |
|--|--------------------|--------------------|-----------|---------|-------------|
| FY4                                    | SD+Met+EtOH        | SD-Met+EtOH        | 0.0300    | 0.8625  | 0.0000      |
| FY4- <i>met15</i> $\Delta$             | SD+Met+EtOH        | SD-Met+EtOH        | 17.2800   | 0.0000  | -0.8926     |
| FY4- <i>met15</i> $\Delta$ ( $\rho$ -) | SD+Met+EtOH        | SD-Met+EtOH        | 12.5952   | 0.0004  | -0.4500     |
| FY4 ( $\rho$ -)                        | SD+Met+EtOH        | SD-Met+EtOH        | 0.4821    | 0.4875  | 0.1471      |
| FY4                                    | SD+Met+Glu         | SD-Met+Glu         | 0.3333    | 0.5637  | 0.0000      |
| FY4- <i>met15</i> $\Delta$             | SD+Met+Glu         | SD-Met+Glu         | 17.2800   | 0.0000  | -0.6168     |
| FY4- <i>met15</i> $\Delta$ ( $\rho$ -) | SD+Met+Glu         | SD-Met+Glu         | 17.2800   | 0.0000  | -0.4874     |
| FY4 ( $\rho$ -)                        | SD+Met+Glu         | SD-Met+Glu         | 3.8533    | 0.0496  | -0.0683     |

**Table S6. *Saccharomyces cerevisiae* strains used in this study (related to Experimental Procedures).**

| Strain #  | Strain name  | Genotype  | Used in Figure(s)  | Source  |
|-----------|--|---|--|---|
| yARC0052  | BY4741   | MAT $\alpha$ <i>his3<math>\Delta</math>1 leu2<math>\Delta</math>0 met15<math>\Delta</math>0 ura3<math>\Delta</math>0</i>  | 1B, 1C, 1D, 1E, 1F, S3, S4A  | Winzeler et al., 1999 (acquired from Horizon Discovery) |
| yARC0053  | BY4742   | MAT $\alpha$ <i>his3<math>\Delta</math>1 leu2<math>\Delta</math>0 lys2<math>\Delta</math>0 ura3<math>\Delta</math>0</i>   | 1B, 1C, 1D, 1E, 1F, S3, S4A  | Winzeler et al., 1999 (acquired from Horizon Discovery) |
| yARC0055  | BY4741 HQ $\Delta$ 0::KanMX                                      | MAT $\alpha$ <i>his3<math>\Delta</math>1 leu2<math>\Delta</math>0 met15<math>\Delta</math>0 ura3<math>\Delta</math>0 HQ<math>\Delta</math>0::KanMX</i>                | S2   | Glaever et al., 2002                                    |
| yARC0056  | BY4742 HQ $\Delta$ 0::KanMX                                      | MAT $\alpha$ <i>his3<math>\Delta</math>1 leu2<math>\Delta</math>0 lys2<math>\Delta</math>0 ura3<math>\Delta</math>0 HQ::KanMX</i>                                     | S2   | Glaever et al., 2002                                    |
| yARC0055a | BY4741 HQ $\Delta$ 0::KanMX + plasmid pBY011                     | MAT $\alpha$ <i>his3<math>\Delta</math>1 leu2<math>\Delta</math>0 met15<math>\Delta</math>0 ura3<math>\Delta</math>0 HQ<math>\Delta</math>0::KanMX pBY011</i>         | S1   | Glaever et al., 2002                                    |
| yARC0055b | BY4741 HQ $\Delta$ 0::KanMX + plasmid pBY011 expressing MET15    | MAT $\alpha$ <i>his3<math>\Delta</math>1 leu2<math>\Delta</math>0 met15<math>\Delta</math>0 ura3<math>\Delta</math>0 HQ<math>\Delta</math>0::KanMX pBY011 (MET15)</i> | S1   | Douglas et. al 2012                                     |
| yARC0083  | FY4  | MAT $\alpha$  | 1G, 2B, 2C, 2D, 2E, 4A, 4B, 4C, 4D, S3, S4A, S4B, S5, S6A, S6B, S8 | Winston et al., 1995                                    |
| yARC0293  | FY4- <i>cys4<math>\Delta</math>0</i>                             | MAT $\alpha$ <i>cys4<math>\Delta</math>0</i>  | 2B, 2C, 2D, S6A, S6B   | This Study  |
| yARC0224  | FY4- <i>met2<math>\Delta</math>0</i>                             | MAT $\alpha$ <i>met2<math>\Delta</math>0</i>  | 2B, 2C, 2D, S6A, S6B   | This Study  |
| yARC0312  | FY4- <i>met3<math>\Delta</math>0</i>                             | MAT $\alpha$ <i>met3<math>\Delta</math>0</i>  | 2B, 2C, 2D, 2E, S5, S6A, S6B                                       | This Study  |
| yARC0458  | FY4- <i>met5<math>\Delta</math>0</i>                             | MAT $\alpha$ <i>met5<math>\Delta</math>0</i>  | 2B, 2C, 2D, S6A, S6B   | This Study  |
| yARC0300  | FY4- <i>met6<math>\Delta</math>0</i>                             | MAT $\alpha$ <i>met6<math>\Delta</math>0</i>  | 2B, 2C, 2D, S6A, S6B   | This Study  |
| yARC0459  | FY4- <i>met10<math>\Delta</math>0</i>                            | MAT $\alpha$ <i>met10<math>\Delta</math>0</i>   | 2B, 2C, 2D, S6A, S6B   | This Study  |
| yARC0222  | FY4- <i>met12<math>\Delta</math>0</i>                            | MAT $\alpha$ <i>met12<math>\Delta</math>0</i>   | 2B, 2C, 2D, S6A, S6B   | This Study  |
| yARC0310  | FY4- <i>met13<math>\Delta</math>0</i>                            | MAT $\alpha$ <i>met13<math>\Delta</math>0</i>   | 2B, 2C, 2D, S6A, S6B   | This Study  |
| yARC0178  | FY4- <i>met15<math>\Delta</math>0</i>                            | MAT $\alpha$ <i>met15<math>\Delta</math>0</i>   | 1G, 2B, 2C, 2D, 2E, 4A, 4B, 4C, 4D, S3, S4A, S4B, S6A, S6B         | This Study  |
| yARC0295  | FY4- <i>str3<math>\Delta</math>0</i>                             | MAT $\alpha$ <i>str3<math>\Delta</math>0</i>  | 2B, 2C, 2D, S6A, S6B   | This Study  |
| yARC0220  | FY4- <i>y0058w<math>\Delta</math>0</i>                           | MAT $\alpha$ <i>y0058w<math>\Delta</math></i>   | S8   | This Study  |
| yARC0414  | FY4- <i>met15<math>\Delta</math>0 y0058w<math>\Delta</math>0</i> | MAT $\alpha$ <i>met15<math>\Delta</math>0 y0058w<math>\Delta</math></i>   |  | This Study  |
| yARC0460  | FY4  | MAT $\alpha$ <i>pGDP-codB::KanMX</i>  | 3D   | This Study  |
| yARC0461  | FY4- <i>met15<math>\Delta</math>0</i>                            | MAT $\alpha$ <i>met15<math>\Delta</math>0 pGDP-codB::KanMX</i>  | 3D   | This Study  |
| yARC0462  | FY4- <i>y0058w<math>\Delta</math>0</i>                           | MAT $\alpha$ <i>y0058w<math>\Delta</math> pGDP-codB::KanMX</i>  | 3D   | This Study  |
| yARC0463  | FY4- <i>met15<math>\Delta</math>0 y0058w<math>\Delta</math>0</i> | MAT $\alpha$ <i>met15<math>\Delta</math>0 y0058w<math>\Delta</math> pGDP-codB::KanMX</i>  | 3D   | This Study  |
| yARC0464  | FY4- <i>met15<math>\Delta</math>0</i>                            | MAT $\alpha$ <i>met15<math>\Delta</math>0 pGDP-y0058w::KanMX</i>  | 3D   | This Study  |
| yARC0465  | FY4- <i>met15<math>\Delta</math>0 y0058w<math>\Delta</math>0</i> | MAT $\alpha$ <i>met15<math>\Delta</math>0 y0058w<math>\Delta</math> pGDP-y0058w::KanMX</i>  | 3D   | This Study  |
| yARC0207  | FY4 ( $\rho$ -)  | MAT $\alpha$ ( $\rho$ -)  | 4D   | This Study  |
| yARC0208  | FY4- <i>met15<math>\Delta</math>0</i> ( $\rho$ -)                | MAT $\alpha$ <i>met15<math>\Delta</math>0</i> ( $\rho$ -)   | 4D   | This Study  |

**Table S7.** Plasmids used in this study (related to **Experimental Procedures**).

| Plasmid #      | Construction   | Yeast Origin | Promoter | Gene Product(s)         | Markers                   | Used in Figure(s) |
|----------------|--|--------------|----------|-------------------------|---------------------------|-------------------|
| pARC0002-MET15 | See (Douglas et al., 2012)   | CEN          | Gal1-10  | MET15                   | URA3                      | S1                |
| pARC0002       | See (Butcher et al., 2006)   | CEN          | Gal1-10  | empty plasmid           | URA3                      | S1                |
| pARC0028       | See (Ryan et al., 2014)  | 2 $\mu$      |          | Cas9+sgRNA              | G418 <sup>R</sup> (KanMX) |                   |
| pARC0112       | LEU2 was replaced by KanMX <sup>R</sup> on plasmid pAG425GPD-ccdB from Yeast Gateway Kit (Alberti et al., 2007)  | 2 $\mu$      | GPD      | ccdB (empty plasmid)    | G418 <sup>R</sup> (KanMX) | 3D                |
| pARC0172       | Made by LR recombination between destination plasmid pARC0112 and entry clone containing the Yll058w gene cds  | 2 $\mu$      | GPD      | Yll058w                 | G418 <sup>R</sup> (KanMX) | 3D                |
| pARC0190       | The coding sequence for MET15 was amplified from <i>S. cerevisiae</i> genomic DNA and cloned into a pET28a-derived vector expressing an N-terminal, cleavable 10XHis-Ruby (Kredel et al., 2009) tag.   |              | T7       | 10XHis-Ruby-TEV-Met15   | Kan <sup>R</sup>          | S10               |
| pARC0191       | The coding sequence for YLL058W was amplified from <i>S. cerevisiae</i> genomic DNA and cloned into a pET28a-derived vector expressing an N-terminal, cleavable 10XHis-Ruby (Kredel et al., 2009) tag. |              | T7       | 10XHis-Ruby-TEV-Yll058w | Kan <sup>R</sup>          | S10               |

**Table S8.** sgRNA, repair fragment template (HR\_template) and amplification primer (HR\_Fw and HR\_rv) sequences used for CRISPR/Cas9-mediated ORF deletions (related to **Experimental Procedures**).

| ORF name | Primers     | Sequence   | Used to construct strain # |
|----------|-------------|--|----------------------------|
| CYS4     | sgRNA       | GTTGTAGGCCACTTGCTCAA   | yARC0293                   |
|          | HR_template | CATCTAGATAAATACGACGTAAGAATAAAAAAAGAACCACGCTTCAAATAAAAGCAAA     |                            |
|          | HR_Fw       | AGTAAAAGGCCAACACTTGAAGATTTTCGTTGTAGGCCACTTGCTCAAACGACATCTAGATA |                            |
|          | HR_Rv       | AGAGAACGGTGCAATTGAATAGGAAAGGAATGACGGATTTTGCTTCTATGTTTGCCTTTTA  |                            |
| MET2     | sgRNA       | ATCGAAAACGGCTCCAAGAGC  | yARC0224                   |
|          | HR_template | AAAGAAAGAAAAAACGTAAGTATAAAAGGAGGATAGATACCACACATACCTCAGGCATAA   |                            |
|          | HR_Fw       | TTTTAGTCACAGGTCCTCCTAAAGTTTCTCTTTATTTGGAATAATAGAAAAAGAA        |                            |
|          | HR_Rv       | GAAAGGACCTCAGTGATGTCATCTACTCTGTCTCTTGCCAAATCGTGCATCCAGTTTA     |                            |
| MET3     | sgRNA       | AACATGCCTGCTCCTCACGG   | yARC0312                   |
|          | HR_template | TAATAATAACAAGAATAAAGTATAATTAACCTGTCATAAAATGCTCCCATCTCAAAGTA    |                            |
|          | HR_Fw       | ACTTATTTGCAAATCTATTTATTTTGC GCGGTCGATCATGAATTTTGCCCTACTTTTGAG  |                            |
|          | HR_Rv       | ACTTATTTGCAAATCTATTTATTTTGC GCGGTCGATCATGAATTTTGCCCTACTTTTGAG  |                            |
| MET5     | sgRNA       | ACAATTGTGGGAGCGTCAAG   | yARC0458                   |
|          | HR_template | TAGTATGCTCTACTATGTCATATGCTATCATCGCCAATCTTTTGTCTCTGTTCC         |                            |
|          | HR_Fw       | AGTTATATTTCAATTGCGAAAAATAAATAAATGTGGGAAGAAAACCAATAGTATGTC      |                            |
|          | HR_Rv       | TTGATATTTATTCAGATCCCTATATACTAATAAAGTAACAGTAGGGAACGGGAACCAGA    |                            |
| MET6     | sgRNA       | TTCAAAGTACATATCAAAAA   | yARC0300                   |
|          | HR_template | ACCAATATAATTTCAAAGTACATATCAAAAGGTTTTAAAAAGGAAGCAAAGTAATGATAT   |                            |
|          | HR_Fw       | ATAAAAAAGCAAGCATCTAAGAGCATTGACAACACTCTAAGAAACAAAATACCAATATAA   |                            |
|          | HR_Rv       | ATTAATCACCAGTGTGAATCCAGAAATAAAAAACAAAAGTTTCAGAAAATATCATTAC     |                            |
| MET10    | sgRNA       | GGATTGGTAGCAAACCTCAAC  | yARC0459                   |
|          | HR_template | TAGATATTTAGTTTTTATTACTATATTAATCTCGTTGTATTTGGGTGACCTCGAGGAA     |                            |
|          | HR_Fw       | AAAAC TAAAGTAAAAAATAAATAAAGTATGTTCAAGACAGGTTCAATAAATAGATATTTA  |                            |
|          | HR_Rv       | TGGAAATAGTTTCGTTTAGATGGGGTGCACATAGTTTTTTCAACTGCTTTCTCGAGG      |                            |
| MET12    | sgRNA       | TCAGAGATTTATATCATGCG   | yARC0222                   |
|          | HR_template | GACGGGACAGGTTGATTACATTTTTTAAACTATTTCACTGAATATAAATACAAAAATGCG   |                            |
|          | HR_Fw       | CTCACATCATCTATTTTGTTCAGTTCTGACATTTTGAAGCGTGTGGACGGGACAG        |                            |
|          | HR_Rv       | TTAGAAGGGCGTTCTGCCGTTATGTATACGTTAAATATTACATTTTTCGCATTTTGG      |                            |
| MET13    | sgRNA       | GAGCAACATAGACAGACCTC   | yARC0310                   |
|          | HR_template | CCACAGTTACTACTACAACCACATCGCAATTAACACAGACAACGATAACAGTTCTTTAAC   |                            |
|          | HR_Fw       | CCTTGATTGAAATAGTCTCCCTAAACTAAAGTTATCAGCAAACAGAACCACCACAGTTAC   |                            |
|          | HR_Rv       | AATGCAATGTAATGTTGAATGTAATGCAAGAGGGGGGGTTGACAAATCTGTTAAAGAAC    |                            |
| MET15    | sgRNA       | GATACTGTTCAACTACACGC   | yARC0178                   |
|          | HR_template | AGATACAATTCATTACCCCATCCATACAGTGTGCGTAATGAGFTGAAAATTATGTAT      |                            |
|          | HR_Fw       | GTCCTTTTCACTACTATTTCTTCGTGTAATACAGGGTCTCAGATACATAGATACAATT     |                            |
|          | HR_Rv       | AATAAAGTTCTGTTTATAAAGTATAGTACTTGTGAGAGAAAGTAGGTTTATACATAATT    |                            |
| STR3     | sgRNA       | CAAGAGATTAGATACAGTTG   | yARC0295                   |
|          | HR_template | agcaaaccaacaagcagcaagcaaaaagGGGAAAATATGCATGTACC#####           |                            |
|          | HR_Fw       | ACATCCCATAGCTCTGTGTGCTTACAGTTTCATT#####caagcaaacac             |                            |
|          | HR_Rv       | TATACTTGACTATTTAAAGTTACTATCTTTGGATTTGAACCTTAT#####             |                            |
| YLL0558W | sgRNA       | TGAACAACTATTAATCATCG   | yARC0220                   |
|          | HR_template | GAACAACATTAATCATCGTGGAAATTATTAGCAGATCATGAGTAGAATATCAAAAAATCA   |                            |
|          | HR_Fw       | TCTCTGGTGCAGTAAACATAAAATTTAAATCTAGTACTCAACCACCACTGAACAACATAT   |                            |
|          | HR_Rv       | TGGAAAAAACTTTTATAAACAATATTTCTATAAAGATTATAAAGAATTCCTGATTTTTGA   |                            |

**Table S9.** Yeast growth conditions in this study (related to **Experimental Procedures**). When required, the analogous liquid medium was made with the same composition, excluding the 2% agar.

| Growth Conditions                 | Composition   | Used in Figure(s)   |
|-----------------------------------|---|---|
| BGGY                              | 10.0 g/L glucose  | 2C, 2D, 4C, S8B, S8C  |
|                                   | 10.0 g/L glycine  |   |
|                                   | 1.0 g/L yeast extract   |   |
|                                   | 3.0 g/L Na <sub>2</sub> SO <sub>4</sub>                                 |   |
|                                   | 2.5 g/L bismuth ammonium citrate  |   |
|                                   | 2 % Agar  |   |
| Homemade YNB – Inorganic Sulfates | 200 $\mu$ L of Vitamin Stock (5000x)                                    | 2E  |
|                                   | 200 $\mu$ L of Trace Elements Stock (10 000x)                           |   |
|                                   | 10 mL of Salt Stock (100x)  |   |
|                                   | 2.0 g/L drop-out  |   |
|                                   | 1 g/L L-glutamic acid   |   |
|                                   | 2 % Glucose/Galactose   |   |
| GNA                               | 2 % agar/agarose  | S2  |
|                                   | 50.0 g/L Glucose  |   |
|                                   | 30.0 g/L Difco Nutrient Broth   |   |
|                                   | 10.0 g/L Yeast Extract  |   |
|                                   | 2 % Agar  |   |
| Homemade YNB + Inorganic Sulfates | 200 $\mu$ L of Vitamin Stock (5000x)                                    | 2E  |
|                                   | 200 $\mu$ L of Trace Elements Stock (10 000x)                           |   |
|                                   | 10 mL of Salt Stock (100x)  |   |
|                                   | 2.0 g/L drop-out  |   |
|                                   | 1 g/L L-glutamic acid   |   |
|                                   | 2 % Glucose/Galactose   |   |
| SC-Leu+Glu                        | 2 % agar/agarose  | S3  |
|                                   | 1.7 g/L Yeast Nitrogen Base without amino acids and ammonium sulfate    |   |
|                                   | 2.0 g/L SC drop-out (-leucine)  |   |
|                                   | 1 g/L L-glutamic acid   |   |
|                                   | 2 % Galactose   |   |
| SC-Met-Cys-Ura+Gal                | 2 % Agar  | S1  |
|                                   | 1.7 g/L Yeast Nitrogen Base without amino acids and ammonium sulfate    |   |
|                                   | 2.0 g/L SC drop-out (-methionine, -cysteine, -uracil)                   |   |
|                                   | 1 g/L L-glutamic acid   |   |
|                                   | 2 % Galactose   |   |
| SC-Met-Cys+Glu                    | 2 % Agar  | 4C, S3  |
|                                   | 1.7 g/L Yeast Nitrogen Base without amino acids and ammonium sulfate    |   |
|                                   | 2.0 g/L SC drop-out (-methionine, -cysteine)                            |   |
|                                   | 1 g/L L-glutamic acid   |   |
|                                   | 2 % Glucose   |   |
| SC-Met-Cys+Gal                    | 2 % Agar  | S3  |
|                                   | 1.7 g/L Yeast Nitrogen Base without amino acids and ammonium sulfate    |   |
|                                   | 2.0 g/L SC drop-out (-methionine, -cysteine)                            |   |
|                                   | 1 g/L L-glutamic acid   |   |
|                                   | 2 % Galactose   |   |
| SD-Met+EtOH                       | 2 % Agar  | 1C, 4D, S4B, S5   |
|                                   | 1.7 g/L Yeast Nitrogen Base without amino acids and ammonium sulfate    |   |
|                                   | 2.0 g/L 'met-cys+ura' drop-out (+histidine, +leucine, +lysine, +uracil) |   |
|                                   | 1 g/L L-glutamic acid   |   |
|                                   | 3 % Ethanol   |   |
| SD-Met+Gal                        | 2 % Agar  | 1C, 3D, S4B, S5   |
|                                   | 1.7 g/L Yeast Nitrogen Base without amino acids and ammonium sulfate    |   |
|                                   | 2.0 g/L 'met-cys+ura' drop-out (+histidine, +leucine, +lysine, +uracil) |   |
|                                   | 1 g/L L-glutamic acid   |   |
|                                   | 2 % Galactose   |   |
| SD-Met+Glu                        | 2 % Agar  | 1B, 1C, 1E, 1F, 1G, 2B, 2E, 4B, 4C, 4D, S2, S4A, S4B, S5, S8A |
|                                   | 1.7 g/L Yeast Nitrogen Base without amino acids and ammonium sulfate    |   |
|                                   | 2.0 g/L 'met-cys+ura' drop-out (+histidine, +leucine, +lysine, +uracil) |   |
|                                   | 1 g/L L-glutamic acid   |   |
|                                   | 2 % Glucose   |   |

|                         |   |                          |
|-------------------------|---|--------------------------|
| SD-Ura+EtOH             | 1.7 g/L Yeast Nitrogen Base without amino acids and ammonium sulfate                  | 1C, S4B, S5              |
|                         | 2.0 g/L '+met-cys-ura' drop-out (+histidine, +leucine, +lysine, +methionine)          |                          |
|                         | 1 g/L L-glutamic acid   |                          |
|                         | 3 % Ethanol   |                          |
|                         | 2 % Agar  |                          |
| SD-Ura+Gal              | 1.7 g/L Yeast Nitrogen Base without amino acids and ammonium sulfate                  | 1C, S4B, S5              |
|                         | 2.0 g/L '+met-cys-ura' drop-out (+histidine, +leucine, +lysine, +methionine)          |                          |
|                         | 1 g/L L-glutamic acid   |                          |
|                         | 2 % Galactose   |                          |
|                         | 2 % Agar  |                          |
| SD-Ura+Glu              | 1.7 g/L Yeast Nitrogen Base without amino acids and ammonium sulfate                  | 1C, S4B, S5              |
|                         | 2.0 g/L '+met-cys-ura' drop-out (+histidine, +leucine, +lysine, +methionine)          |                          |
|                         | 1 g/L L-glutamic acid   |                          |
|                         | 2 % Glucose   |                          |
|                         | 2 % Agar  |                          |
| SD-Leu+Glu              | 1.7 g/L Yeast Nitrogen Base without amino acids and ammonium sulfate                  | S4B                      |
|                         | 2.0 g/L '+met-cys-leu' drop-out (+histidine, +uracil, +lysine, +methionine)           |                          |
|                         | 1 g/L L-glutamic acid   |                          |
|                         | 2 % Glucose   |                          |
|                         | 2 % Agar  |                          |
| SD+Met+EtOH             | 2.0 g/L '+met-cys-ura' drop-out (+histidine, +leucine, +lysine, +methionine)          | 4D                       |
|                         | 1 g/L L-glutamic acid   |                          |
|                         | 2 % Glucose   |                          |
|                         | 2 % Agar  |                          |
|                         | 2 % Agar  |                          |
| SD+Met+Glu              | 1.7 g/L Yeast Nitrogen Base without amino acids and ammonium sulfate                  | 1C, 2E, 4D, S4A, S4B, S5 |
|                         | 2.0 g/L '+met-cys-ura' drop-out (+histidine, +leucine, +lysine, +uracil, +methionine) |                          |
|                         | 1 g/L L-glutamic acid   |                          |
|                         | 2 % Glucose   |                          |
|                         | 2 % Agar  |                          |
| SD+Met+Bi+Glu           | 1.7 g/L Yeast Nitrogen Base without amino acids and ammonium sulfate                  | S6A, S6B, S6B, S6C       |
|                         | 2.0 g/L '+met-cys-ura' drop-out (+histidine, +leucine, +lysine, +uracil)              |                          |
|                         | 1 g/L L-glutamic acid   |                          |
|                         | 2 % Glucose   |                          |
|                         | 2 % Agar  |                          |
|                         | 2.5 g/L bismuth ammonium citrate  |                          |
| SPO                     | 1.25 g/L Yeast Extract  | S2                       |
|                         | 10.0 g/L Potassium Acetate  |                          |
|                         | 20 g/L Peptone  |                          |
| YPDA                    | 10 g/L Yeast Extract  | 2B, 4C, S6A              |
|                         | 2 % Glucose   |                          |
|                         | 120 mg/L Adenine  |                          |
|                         | 2 % Agar  |                          |
|                         |   |                          |
| SC-Met-Cys+(Fe)EDTA+Glu | 1.7 g/L Yeast Nitrogen Base without amino acids and ammonium sulfate                  | 4C, S2                   |
|                         | 2.0 g/L SC drop-out (-methionine, -cysteine)  |                          |
|                         | 1 g/L L-glutamic acid   |                          |
|                         | 2 % Glucose   |                          |
|                         | 2 % Agar  |                          |
|                         | 0.048M Fe-EDTA  |                          |
| SD-Met+(Fe)EDTA+Glu     | 1 g/L L-glutamic acid   | 4B                       |
|                         | 2 % Glucose   |                          |
|                         | 2 % Agar  |                          |
|                         | 0.048M Fe-EDTA  |                          |

| <b>Homemade Yeast Nitrogen Base without Inorganic Sulfate</b> |                      |               |
|---|----------------------|---------------|
| <b>Component</b>  | <b>Concentration</b> | <b>Amount</b> |
| <b>Vitamins (1 Liter Stock, 5000x)</b>                        |                      |               |
| Biotin  | 2µg/L                | 0.010g        |
| Calcium Pantothenate  | 400µg/L              | 2.000g        |
| Folic Acid  | 2µg/L                | 0.010g        |
| Inositol  | 2,000µg/L            | 10.000g       |
| Niacin  | 400µg/L              | 2.000g        |
| p-Aminobenzoic Acid   | 200µg/L              | 1.000g        |
| Pyridoxine Hydrochloride                                      | 400µg/L              | 2.000g        |
| Riboflavin  | 200µg/L              | 1.000g        |
| Thiamine Hydrochloride  | 400µg/L              | 2.000g        |
| <b>Trace Elements (1 Liter Stock)</b>                         |                      |               |
| Boric Acid  | 500µg/L              | 2.500g        |
| Cupric chloride   | 37.74µg/L            | 0.189g        |
| Potassium Iodide  | 100µg/L              | 0.500g        |
| Ferric Chloride   | 200µg/L              | 1.000g        |
| Manganese Chloride  | 333.34µg/L           | 1.667g        |
| Sodium Molybdate  | 200µg/L              | 1.000g        |
| Zinc Sulfate  | 400µg/L              | 2.000g        |
| <b>Salts (1 Liter Stock, 100x)</b>                            |                      |               |
| Monopotassium Phosphate                                       | 1.0g/L               | 100.0g        |
| Magnesium Chloride  | 0.395g/L             | 39.5g         |
| Sodium Chloride   | 0.1g/L               | 10.0g         |
| Calcium Chloride  | 0.1g/L               | 10.0g         |

| <b>Homemade Yeast Nitrogen Base with Inorganic Sulfate</b> |                      |               |
|--|----------------------|---------------|
| <b>Component</b>   | <b>Concentration</b> | <b>Amount</b> |
| <b>Vitamins (1 Liter Stock, 5000x)</b>                     |                      |               |
| Biotin   | 2µg/L                | 0.010g        |
| Calcium Pantothenate                                       | 400µg/L              | 2.000g        |
| Folic Acid   | 2µg/L                | 0.010g        |
| Inositol   | 2,000µg/L            | 10.000g       |
| Niacin   | 400µg/L              | 2.000g        |
| p-Aminobenzoic Acid  | 200µg/L              | 1.000g        |
| Pyridoxine Hydrochloride                                   | 400µg/L              | 2.000g        |
| Riboflavin   | 200µg/L              | 1.000g        |
| Thiamine Hydrochloride                                     | 400µg/L              | 2.000g        |
| <b>Trace Elements (1 Liter Stock)</b>                      |                      |               |
| Boric Acid   | 500µg/L              | 2.500g        |
| Copper Sulfate   | 40µg/L               | 0.200g        |
| Potassium Iodide   | 100µg/L              | 0.500g        |
| Ferric Chloride  | 200µg/L              | 1.000g        |
| Manganese Sulfate  | 400µg/L              | 2.000g        |
| Sodium Molybdate   | 200µg/L              | 1.000g        |
| Zinc Sulfate   | 400µg/L              | 2.000g        |
| <b>Salts (1 Liter Stock, 100x)</b>                         |                      |               |
| Monopotassium Phosphate                                    | 1.0g/L               | 100.0g        |
| Magnesium Sulfate  | 0.5g/L               | 50.0g         |
| Sodium Chloride  | 0.1g/L               | 10.0g         |
| Calcium Chloride   | 0.1g/L               | 10.0g         |

## SUPPLEMENTARY REFERENCES

- Alberti, S., Gitler, A.D., and Lindquist, S. (2007). A suite of Gateway cloning vectors for high-throughput genetic analysis in *Saccharomyces cerevisiae*. *Yeast* *24*, 913-919. 10.1002/yea.1502.
- Butcher, R.A., Bhullar, B.S., Perlstein, E.O., Marsischky, G., LaBaer, J., and Schreiber, S.L. (2006). Microarray-based method for monitoring yeast overexpression strains reveals small-molecule targets in TOR pathway. *Nat Chem Biol* *2*, 103-109. 10.1038/nchembio762.
- Douglas, A.C., Smith, A.M., Sharifpoor, S., Yan, Z., Durbic, T., Heisler, L.E., Lee, A.Y., Ryan, O., Gottert, H., Surendra, A., et al. (2012). Functional analysis with a barcoder yeast gene overexpression system. *G3 (Bethesda)* *2*, 1279-1289. 10.1534/g3.112.003400.
- Giaever, G., Chu, A.M., Ni, L., Connelly, C., Riles, L., Veronneau, S., Dow, S., Lucau-Danila, A., Anderson, K., Andre, B., et al. (2002). Functional profiling of the *Saccharomyces cerevisiae* genome. *Nature* *418*, 387-391. 10.1038/nature00935.
- Kredel, S., Oswald, F., Nienhaus, K., Deuschle, K., Rocker, C., Wolff, M., Heilker, R., Nienhaus, G.U., and Wiedenmann, J. (2009). mRuby, a bright monomeric red fluorescent protein for labeling of subcellular structures. *PLoS One* *4*, e4391. 10.1371/journal.pone.0004391.
- Lu, H., Li, F., Sanchez, B.J., Zhu, Z., Li, G., Domenzain, I., Marcisauskas, S., Anton, P.M., Lappa, D., Lieven, C., et al. (2019). A consensus *S. cerevisiae* metabolic model Yeast8 and its ecosystem for comprehensively probing cellular metabolism. *Nat Commun* *10*, 3586. 10.1038/s41467-019-11581-3.
- Winston, F., Dollard, C., and Ricupero-Hovasse, S.L. (1995). Construction of a set of convenient *Saccharomyces cerevisiae* strains that are isogenic to S288C. *Yeast* *11*, 53-55. 10.1002/yea.320110107.

Winzeler, E.A., Shoemaker, D.D., Astromoff, A., Liang, H., Anderson, K., Andre, B., Bangham, R., Benito, R., Boeke, J.D., Bussey, H., et al. (1999). Functional characterization of the *S. cerevisiae* genome by gene deletion and parallel analysis. *Science* 285, 901-906.  
10.1126/science.285.5429.901.